Raising the bar in seismic design

cost–benefit analysis of alternative design methodologies and earthquake-resistant technologies

Ciurlanti, Jonathan; Bianchi, Simona; Pampanin, Stefano

DOI
10.1007/s10518-023-01625-x

Publication date
2023

Document Version
Final published version

Published in
Bulletin of Earthquake Engineering

Bulletin of Earthquake Engineering
https://doi.org/10.1007/s10518-023-01625-x

ORIGINAL ARTICLE

Raising the bar in seismic design: cost–benefit analysis of alternative design methodologies and earthquake-resistant technologies

Jonathan Ciurlanti[1] · Simona Bianchi[2] · Stefano Pampanin[3]

Received: 10 July 2022 / Accepted: 18 January 2023

Abstract
The severe socio-economic impact of recent earthquakes has represented a tough reality check, further confirming the mismatch between society expectations and reality of seismic performance of modern buildings. Life-safety code-compliant design criteria are not enough when dealing with new structures. To raise the bar in terms of structural safety and overall performance objectives, the renewed challenge is defining high-performance buildings able to sustain a design-level earthquake with minimum disruption of business and limited economic losses. To achieve this goal, alternative strategies might be adopted: (a) implementing more advanced design methodologies, (b) increasing the seismic design level, (c) adopting low-damage earthquake-resistant technologies. However, the common perception is that these strategies would lead to unaffordable costs. To support decision-makers, the paper develops a comprehensive parametric study to compare the cost–benefit of reinforced concrete multi-storey buildings designed for increasing levels of seismic intensities (representing a higher seismicity zone or Importance Class) and according to alternative design approaches (Force-based vs. Displacement-based) and technologies (traditional vs. low-damage). Analytical/numerical investigations are carried out to determine the building performance, and loss assessment analyses are performed to compute the Expected Annual Losses of all the parametric configurations. Results, further elaborated through a machine-learning technique, highlight the convenience of implementing more advanced design methodologies, such as a displacement-based approach allowing for a better control of the building response, and the remarkable benefits of applying low-damage technologies, leading to a very high performance and significantly reduced economic losses ($>50\%$) for a small increase (<5–10%) of the initial investment cost.

Keywords Seismic safety · Seismic design · Performance-based · Force-based · Displacement-based · Low damage · Economic losses

✉ Jonathan Ciurlanti
jonathan.ciurlanti@arup.com

[1] ARUP, Amsterdam, The Netherlands

[2] Department of Structural Design and Mechanics, Delft University of Technology, Delft, The Netherlands

[3] Department of Structural and Geotechnical Engineering, Sapienza University of Rome, Rome, Italy

Published online: 01 February 2023

1 Introduction

Lessons from recent seismic events have further confirmed the unexploited potentialities as well as the actual implementation limits of the current performance-based seismic design philosophy for reinforced concrete buildings. Although modern multi-storey structures performed as expected from a technical point of view, concentrating the inelastic demand in discrete plastic hinges zones as per hierarchy of strengths or capacity design principles, they were severly damaged after earthquakes and considered too expensive to be repaired, requiring demolition in many cases (Verderame et al. 2009; Ricci et al. 2011; Kam et al. 2011; Wallace et al. 2012). This led to substantial socio-economic losses in terms of both repair costs and business interruption, in addition to a massive negative impact on the environment. Furthermore, a significant portion of the post-earthquake economic losses is related to the damage of non-structural elements (O'Reilly et al. 2018), typically neglected in the seismic design in spite of their inherently high vulnerability and capital investment when compared to the structural cost (Whittaker and Soong 2003). Severe damage to buildings after major earthquakes cannot be acceptable anymore, therefore, Life-Safety design criteria are not enough when dealing with new building design (Pampanin 2012, 2015).

As a matter of fact, in recent years research studies have been focusing on raising the bar in seismic design towards enhanced seismic safety and performance levels for our modern structures (Kasai et al. 2009; Ricles et al. 2010; FEMA P-58–7 2018). The goal is creating stronger, safer and more resilient communities, thus avoiding severe post-earthquake consequences in terms of socio-economic losses. To achieve this, either an improved or advanced design methodology and/or a high-performance (low-damage) earthquake-resistant technologies could be employed, leading to more sustainable impact/consequences with the possible (but not necessarily required in all cases) trade-off of slighlty higher initial cost (Fig. 1).

In order to develop and employ a high-performance building able to sustain a design level earthquake with limited damage, seismic design philosophies and technologies need to move towards a more appropriate damage-control approach embracing the entire building system, including structural skeleton and building envelope. Within this context, in the past twenty years, growing attention has been, dedicated to either: (1) design methods

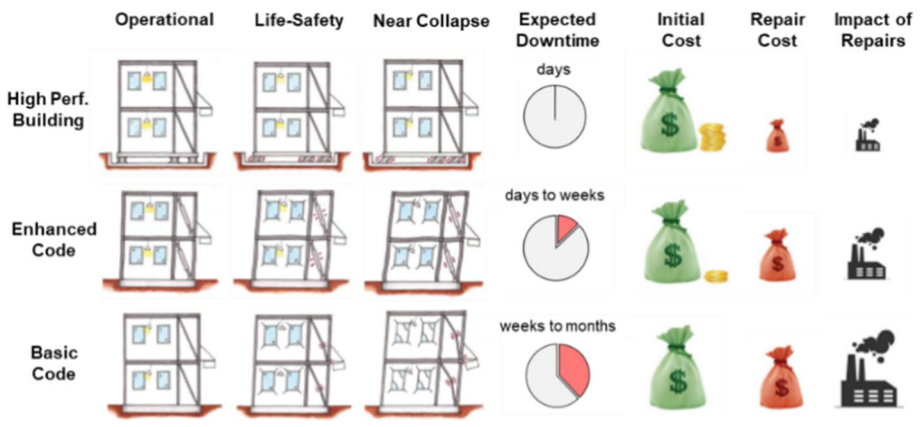

Fig. 1 Earthquake consequences associated with alternative design strategies (modified after FEMA P-58–7 2018)

based on displacements rather than forces, providing a better control of the building behaviour in the inelastic domain (Priestley 1998; Priestley and Kowalsky 2000; Priestley et al. 2007), and/or (2) the development of damage-mitigation technologies, aiming at the reduction of the post-earthquake damage. Beyond the more traditional and well-known advanced technologies such as base isolation and dissipative braces, particular interest has being received by the so-called "low-damage" systems, based on post-tensioned rocking dissipative mechanisms, i.e. the PRESSS technology (PREcast Seismic Structural System) for concrete structures (Priestley 1991; Priestley et al. 1999; Pampanin 2005, Pampanin et al. 2010). This moment-resisting solution combines self-centering capacity, through post-tensioned bars/tendons in the structural members, with dissipation capabilities, provided either by internally located mild steel bars, as per the first generation of the technology, or by externally replaceable *Plug&Play* dissipaters, more recently developed (Pampanin 2005; Marriott et al. 2008, Sarti et al. 2016). The system behavior results in a dissipative and re-centering *Flag-Shape* hysteresis behaviour (fib 2003) allowing for negligible permanent deformations after earthquakes. Furthermore, the low-damage philosophy has been recently applied to non-structural elements, often neglected in seismic design procedures despite being the most vulnerable and expensive components in a building system (Taghavi and Miranda 2003). The seismic behavior of traditional non-structural elements (facades, partitions and ceilings) can be easily improved by introducing simple details modifications, as internal gaps within adjacent sliding interfaces and/or dissipative devices (e.g. Baird et al. 2013; Tasligedik et al. 2015; Tasligedik and Pampanin 2016; Dhakal et al. 2016; Brandolese et al. 2019; Bianchi et al. 2021; Ciurlanti et al. 2022; Bianchi and Pampanin 2022), without significantly increase the labor and material costs.

Nevertheless, a common obstacle to the wider application of advanced seismic design methodologies and innovative low-damage technologies is often the uninformed perception that these would lead to substantially higher costs. Moreover, the actual economic benefits associated with a reduced level of damage, consequently reduced post-earthquake economic losses, are rarely computed. This paper intends to shed a light on this topic by providing robust evidences for informed decision-making on the opportunity and solutions to raise the bar towards more resilient communities. Specifically, this research fits into the context of society's growing need for safer and more resilient buildings and the novelty of this work is associated with the quantification of the beneficial effects of designing in a more conscious and controlled way (in terms of reduction of direct economic losses and increase of related savings). This objective is pursued through a parametric study to compare the cost/performance of case-study buildings considering different design parameters, design methods and/or construction technologies. A summary of the alternative design/technological strategies investigated within this work is presented in Fig. 2 and detailed discussed in the following section.

2 Research outline

As part of the parametric investigation, alternative analytical design methods are employed, i.e. the traditional Force-Based Design (FBD) and the more advanced Direct Displacement-Based Design (DDBD or DBD), in order to highlight that by targeting and thus controlling/limiting displacements rather than forces allows to better control the performance of buildings in the non-linear (plastic) range. The FBD procedure, herein implemented following

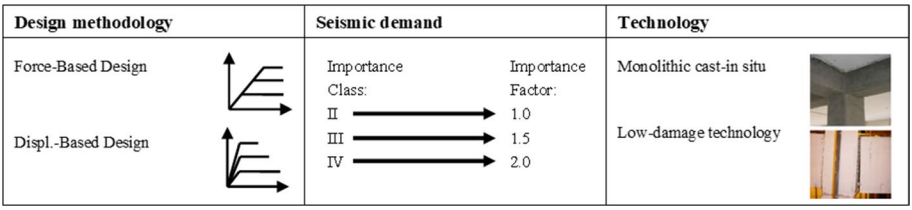

Fig. 2 Summary of enhanced-resilient strategies involved in this study: alternative design methodologies (Forced-Based vs. Displacement Based), Importance Levels/Classes, traditional vs. low-damage technologies

the equivalent static approach as per the prescriptions of the Italian code (NTC 2018), can be adopted when the building is within certain constraints (e.g. regularity in plan and elevation), and is based on the calculation (better rough estimation) of the first natural period of the structure by alternative formulations and on the selection of a behaviour factor (q) depending on the structural typology, its statically indeterminate level and the ductility class. Worth reminding that the same methodology and related formulations are included in the Eurocode 8 (EN 1998–1 2004). Critical shortcomings related to this methodology have been discussed by Priestley (2003), Sullivan (2013) who showed that a number of key assumptions do not allow to properly control the building structural behaviour in the plastic domain, since the method inherently assumes that the stiffness is constant and thus independent from the structure's strength. This means that the yield curvature would be directly proportional to strength while basics of structural design as well as detailed analyses and experimental evidence proved the inconsistency of this assumption for RC structures (Priestley 2003). More recently, Sporn and Pampanin (2013) proposed a "retrofit" strategy for the FBD approach, where the design methodology is corrected and refined by introducing an iterative or, even better, a closed-form solution to respect the stiffness-strength compatibility relationship. In the same study, it is also highlighted that the predominant natural period of the building should be taken as the secant-to-yielding period of the equivalent elasto-plastic system rather than be estimated by empirical formulations.

On the other hand, the DDBD method (Priestley 1998; Priestley et al. 2005, 2007) is based on the initial choice of a target drift, therefore the seismic behaviour/performance of the structure is controlled upfront by the designer and his/her design choice, then material strain limits and global displacements/drifts are directly controlled.

It is worth mentioning that the energy-based approach (Fardis 2018, Benavent-Climent et al. 2021) is not investigated in this study that focuses on code-compliant procedures. However, although modern seismic codes suggest force and/or displacement-based design methodologies, it is acknowledged that these procedures do not account for duration related cumulative damage and frequency content of the earthquake record which can be captured through an energy-based approach.

In addition to the two different design methodologies, the enhancement of the seismic safety level is studied through the variation of the Importance Level or Class of the building (II, III, IV, i.e. from ordinary to strategic buildings), leading to a consequent increase of the seismic demand (design) level. In practice, this means that the buildings are firstly designed with the minimum-by-code assigned to ordinary residential or office structures, then with a higher importance level corresponding to strategic structures such as hospitals, police station, etc. According to the NTC 2018, the variation of the Importance Level/Class involves a different coefficient representing the Importance/Use Factor (C_u), affecting

the Reference Period (V_R) of the building, and consequently the Return Period (T_R) of the seismic demand at different limit states. Practically, this coefficient modifies the design spectra.

In terms of technologies, two different types of structural connections are studied: (1) a traditional cast-in-situ system and (2) a low-damage PRESSS solution (Priestley 1991; Priestley et al. 1999). The traditional monolithic connections adopt B450 C steel rebars and C45/55 concrete and are designed following the NTC 2018 provisions, while the hybrid connections consist of external *Plug&Play* dissipative devices (Pampanin 2005; Newcombe at al. 2008; Sarti et al. 2016) in combination with unbonded post-tensioned tendons/bars. The low-damage system (Fig. 3) develops a controlled rocking motion during the earthquake shakings, reducing the residual inter-story drift due to the re-centering effect of the unbonded post-tensioned tendons. Specifically, following a proper design procedure, the precast elements start "rocking" against each other and return to the initial position showing no permanent deformations. This means that the structural skeleton remains basically undamaged after a design-level earthquake with very limited repair costs and time, as also computed by Bianchi et al. (2020), with the only repairing actions possibly consisting of the simple substitution of the (damaged) external replaceable dissipaters. Furthermore, dry jointed precast connections provide for significant advantages in the construction phases, with increasing quality control, erection speed as well as safe and clean work areas as well as during, or at the end of, the life-span of the building, with modular demountability and possibility to relocate/recycle components or entire portions of the building.

Considering all these alternative design strategies, a set of parametric building configurations is identified as discussed in the next section. Analytical and numerical investigations are therefore developed to analyse the building performance of all case studies. For each configuration, construction costs (material and labour costs) are also computed to determine the initial cost of the alternative solutions. Finally, loss assessment analyses are performed to estimate the Expected Annual Losses (EAL) following the probabilistic-based procedure described in FEMA P-58–1 (2018). Results are finally compared for all the configurations in terms of seismic costs at the end of the building service life (50 years). This long-term view (minimum-by-law ordinary building life span, e.g. 50 years) represents a valuable information for the purpose of the

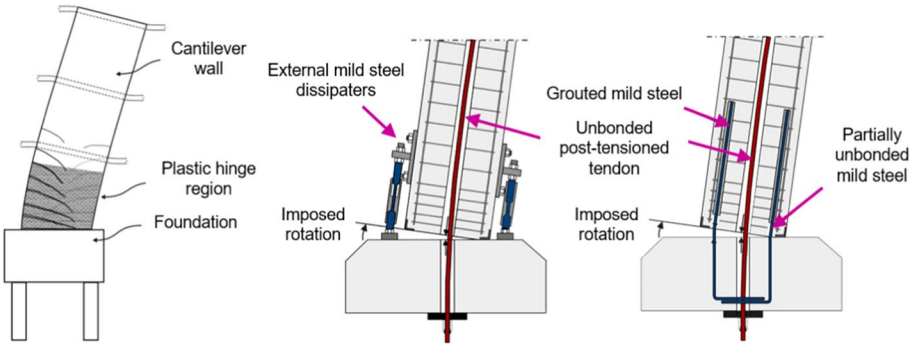

Fig. 3 Comparative response of a traditional monolithic system (left) and a jointed precast solution with internal (centre) and external (right) dissipaters/fuses (modified after fib 2003; Marriott et al. 2008)

economic comparison, proving that designing for higher levels of safety and resilience is indeed cost-effective and not only beneficial from a seismic performance point of view. Furthermore, parametric results are further elaborated through a machine-learning technique to identify the best design ductility range (and inter-storey drift) leading to target EALs lower than 0.5%. This means that the building would be expected to belong to the safest risk class A^+, as per DM 58 (2017) prescriptions. This approach can be implemented as part of the design of such innovative low-damage structures, in order to make appropriate design choices towards cost-efficient safer levels at the very early stage of the design process.

2.1 Python-based workflow

Lately, the development of digital tools/workflows and automation have had a remarkable impact in terms of both speeding up the iterative design process and getting further insights from projects. In order to automate the simulation process of this research work, an effective Python-based workflow has been developed to perform the large number of parametric analyses (24,300 simulations) and manipulate the datasets involved in this study. A workflow consists of a series of activities that need to be executed in order to achieve a desired outcome, and each activity represents an automated step, taking a set of inputs and producing a set of outputs. The workflow, based on object-oriented programming, considers Python modules and submodules working either as standalone or within a series of automated routines, making the tool flexible and scalable. A schematic drawing of the workflow is shown in Fig. 4.

The user can initially define the parametric building models, through their geometrical and material properties, directly in Grasshopper, a visual programming language and environment incorporated in Rhinoceros 3D (McNeel et al. 2010). The Outputs,

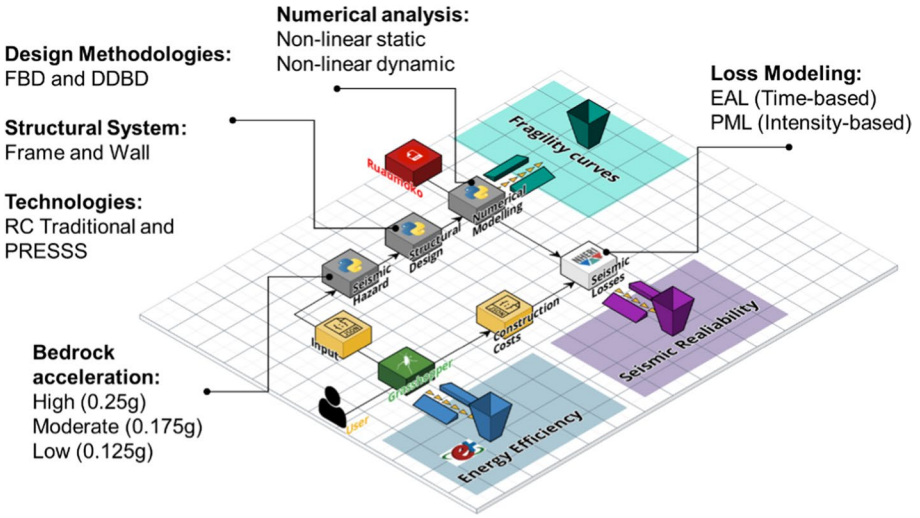

Fig. 4 Automated workflow developed in Python: from hazard level to selection of input recorded motion, to FBD or DDBD design, to numerical analysis and loss modeling

in the form of.*json* files (objects), containing all the building information, (e.g. number of spans and floors, global and section dimensions, floor masses, type of analysis and its settings) are collected from the parametric model. Also, construction costs are automatically computed in Grasshopper based on element volumes and labor costs and stored in a.*json* file (object) subdivided into different component families. In a workflow perspective, these files are the Input data for the automated workflow.

Herein, a summary of the main workflow activities involving different modules and sub-modules running in series, namely:

- *Seismic Hazard* The user can select among different seismic hazard levels and other hazard related properties, i.e. soil type (A, B, C, D, E), Importance Class (I, II, III and relative C_u), and service building life ($\underline{V}_n$). Nine elastic acceleration and displacement design spectra referring to different limit states (depending on T_R) are developed as main outcomes of this module. Furthermore, a scaling procedure, based on NZS 1170.5 (2004), is also included to possibly obtain a set of scaled spectrum-compatible accelerograms for each intensity level based on the European Strong-motion Database.
- *Structural Design* Two alternative analytical design methodologies are implemented: FBD and DDBD. Regarding the selection of the key design parameters, such as the behavior factor (q) for FBD and the design drift θ_d for DDBD, respectively, it is possible either to define a single user-selected value, or to specify a discrete number of samples representing the entire ductility range within two boundary conditions: (1) minimum ductility (e.g. $\mu = q = 1.5/2$) and (2) maximum design inter-storey drift (e.g. 2%). Moreover, two different solutions for both the structural system (frames or walls) and its technology (monolithic or PRESSS) are included.
- *Numerical Modelling*. Input text files for Ruaumoko 2D software (Carr 2003) are automatically generated right after the connection design. Either non-linear push-over (NLPO) or non-linear time history (NLTH) analyses can be carried out with or without considering the explicit modelling of non-structural elements (sole bare frame and/or integrated system). This module involves the creation of a batch file to run the analyses and the post-processing of the results. Engineering demand parameters (floor displacements and floor accelerations) are then manipulated and stored in a data frame easily readable from subsequent activities.
- *Seismic Losses*. Following the FEMA P-58–1 (2018) probabilistic methodology, two different loss modelling approaches, either time-based and intensity-based, are implemented in the workflow: (1) the estimation of the EAL and 2) the evaluation of the Probable Maximum Losses (PML). The *pelicun* framework, developed by Zsarnóczay and Deierlein (2020) within an open source and publicly available Python library, has been integrated in the existing workflow to quantify the post-earthquake repair costs.

By combining the user-defined values/properties and the Python-based activities previously described, a comprehensive set of different outcomes can be obtained. In this specific study, the simulation outputs are used to compare the alternative resilient-enhancing strategies discussed above.

It is worth mentioning that the Python-based workflow also accounts for the possibility of implementing energy dynamic simulations for the building, thus energy efficiency analyses by using the input file generated in Grasshopper. However, this module

is not adopted for this specific research work while an example of its application is shown in Bianchi et al. (2022).

3 Parametric cost/performance-based investigation

For this specific study a 5-story Reinforced Concrete (RC) building with global dimensions as indicated in Fig. 5 is selected, by referring to a mock-up building already analysed in a previous research work by the same authors (Bianchi et al. 2020). The structural skeleton consists of moment-resisting frames (beams: 0.40 m × 0.75 m; columns: 0.75 m × 0.4 m) in the X- direction and structural walls (0.40 m × 6 m) in the orthogonal Y-direction as seismic resisting systems, while the other elements carry the self-weight loads only. The first two building floors have residential use, while the other two are offices; the roof top is considered not accessible. The flooring system consists of hollow core slabs (0.25 m thick, one-way spanning) and the total seismic mass is around 658 tons and 520 tons for a typical floor and the roof level, respectively.

Different typologies of non-structural components are also investigated, specifically: two types of external enclosures (precast concrete claddings and stick-built curtain in the frame and wall direction, respectively), steel framed drywall gypsum partitions, fully floating suspended ceilings and all the required building services and contents. Although these components are included as weight and mass in the seismic design, as well as they are all considered in the loss modelling in terms of fragility functions, in this investigation their explicit modelling is neglected assuming low interaction between the primary structure and non-structural elements. Moreover, in this specific study, traditional construction practice details are considered for the non-structural components, meaning that the "low-damage" structure involves the bare frame system only.

The parametric building configurations are identified by taking into account (1) three different low-to-high seismicity zones, whose main parameters are summarized in Table 1

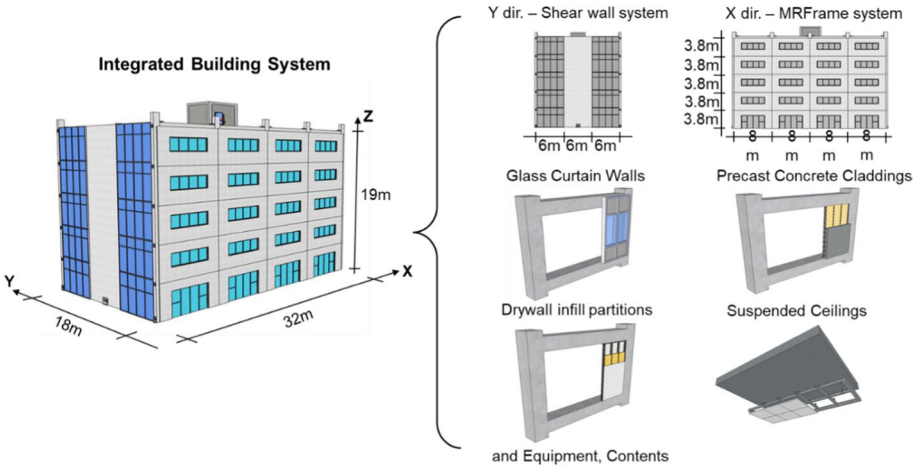

Fig. 5 Reinforced Concrete (RC) case study building

Table 1 Design hazard parameters for all the seismicity levels (low-to-high) and Importance Classes (II, III, IV) considered in this investigation

	Low seismicity			Moderate seismicity			High seismicity		
C_u, importance factor	1	1.5	2	1	1.5	2	1	1.5	2
V_n [yr], service building life	50	50	50	50	50	50	50	50	50
T_R [yr], return period	475	712	949	475	712	949	475	712	949
ag [g], PGA on soil type A	0.125	0.14	0.16	0.175	0.20	0.22	0.25	0.29	0.33
S, Soil factor	1.5	1.48	1.46	1.44	1.40	1.37	1.34	1.29	1.23
PGA [g], peak ground Acc	0.19	0.21	0.23	0.25	0.28	0.30	0.33	0.37	0.40
F_0, amplification factor	2.55	2.55	2.56	2.47	2.48	2.48	2.38	2.39	2.40
T_d [s], corner period	2.10	2.16	2.23	2.30	2.40	2.49	2.60	2.76	2.91

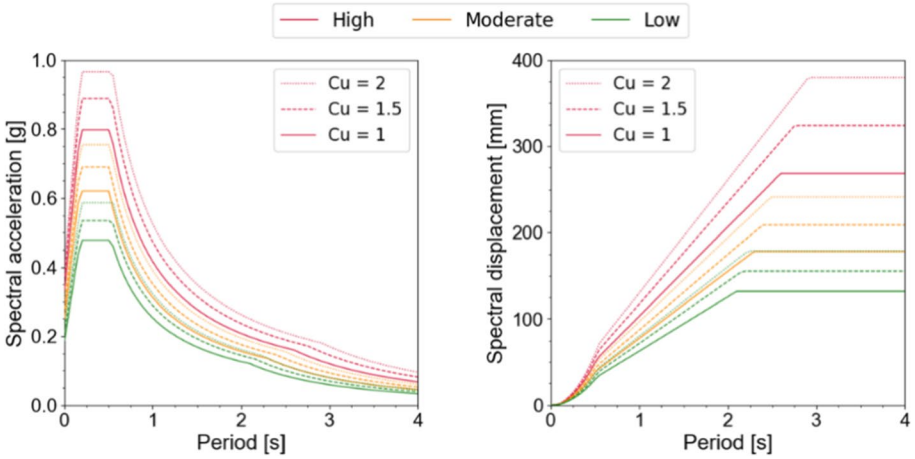

Fig. 6 Acceleration and displacement elastic design spectra for the design level earthquakes

for the design level earthquake (10% probability of exceedance in 50 years), as well as (2) the three Importance Levels/Classes included in NTC 2018, providing a coefficient C_u (1.0, 1.5, 2.0) which increases the seismic demand when compared to the reference benchmark I2 class for residential buildings (Fig. 6), effectively increasing the Return Period T_R and thus reducing the probability of exceedance in V_n. Therefore, a total of 9 hazard values (seismic scenarios) are involved in this investigation.

3.1 Seismic design methodologies

A total of 27 parametric building configurations (design values are listed in Appendix-Table 5) are employed, involving two design methodologies, FBD vs. DDBD (Fig. 7), and two different technologies for the structural systems (monolithic cast-in situ vs. PRESSS for both frames and walls), as discussed above (9 hazard values—Table 1 - x 3 buildings: FBD—Traditional, DDBD—Traditional, DDBD—Low Damage). Specifically, the

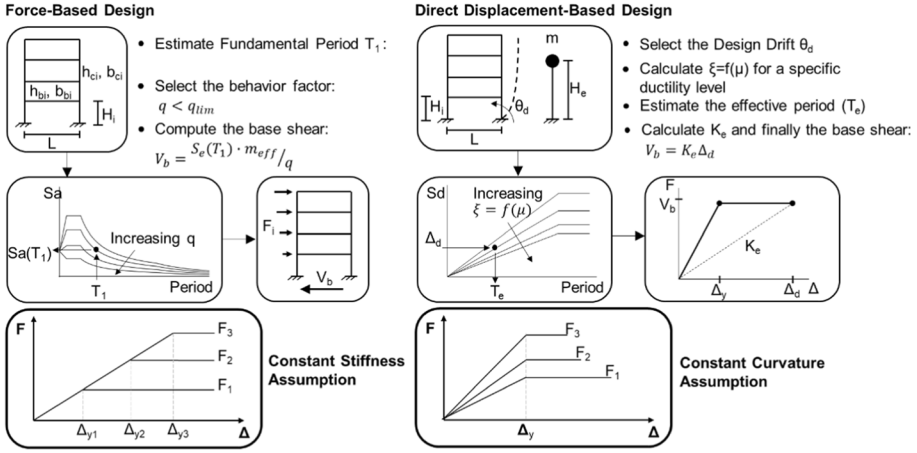

Fig. 7 Schematic flow chart of FBD (left) vs. DDBD (right) procedure

traditional buildings are designed following both FBD and DDBD approaches and referring to the prescriptions provided by NTC (2018) and Priestley et al. (2007), respectively. A modified DDBD procedure, specific for low-damage structures (Pampanin et al. 2010), is instead implemented to design the hybrid (PRESSS) connections.

Following the FBD equivalent static procedure described in NTC (2018), as well as in EN 1998–1 (2004), the design acceleration response spectra at ULS are obtained from the 5% elastic spectra properly scaled by the behavior factor (q). The total base-shear (V_b) is therefore calculated by multiplying the spectral acceleration at the first natural period of the structure, S_a (T_1), where T_1 can be computed in function of the building height (H) and a coefficient (C) based on the structural typology, and the building mass (reduced by a coefficient $\lambda = 0.85$ to determine the effective mass), divided by the behaviour factor (q):

$$T_1 = CH^{3/4} \tag{1}$$

$$V_b = S_e(T_1) \cdot (mass \cdot \lambda)/q = S_e(T_1) \cdot mass_{eff}/q \tag{2}$$

Displacements at ULS are verified at the end of the design process by multiplying the elastic displacements of the structure, obtained by pushing the building with external forces representing the distribution of the base shear along the building height, and its ductility.

On the contrary, displacements are key parameters and lead the design in the DDBD procedure (Priestley et al. 2007). Displacements of the building are controlled by assuming appropriate inter-story drift limits, as suggested by design codes, good practice and/or material strain limits. The design procedure consists of determining an equivalent building Single Degree of Freedom (SDOF) system, with effective secant stiffness (K_e), effective mass (m_e), effective height (H_e) and equivalent viscous damping (ξ_e) related to the target displacement (Δ_d) selected. By reducing the 5% damped design spectrum to account for

the ductility/damping of the system, the effective period can be defined (T_e) from the target displacement. Then, the building base shear can be easily computed (V_b).

$$K_e = 4\pi^2 m_e / T_e^2 \tag{3}$$

$$V_b = K_e \Delta_d \tag{4}$$

The entire range of possible design ductility is explored for all 27 parametric configurations, assuming for the monolithic structure designed following both design approaches to have the same ductility value $q = \mu_{FBD,i} = \mu_{DBD,i}$. The study involves on average 10 ductility values for each building configuration leading to a large range of design displacements/drifts and q factors to develop the parametric analysis.

Furthermore, the seismic design is implemented and carried out referring to material characteristic, 5th percentile, values without accounting for material partial reduction factors or other safety factors in order to achieve a better comparison between the analytical and numerical results. Figure 8 presents the analytical capacity curves obtained for the frame direction in case of high seismicity and Importance Class II. The different assumptions at the base of both design methods can be highlighted: (1) FBD is characterized by an initial elastic stiffness, and the different base shears are identified by varying the behaviour factor q; (2) DDBD considers the initial stiffness directly linked with the structure strength, decreasing when the base shear decreases. Moreover, an initial higher ductility is considered for the low-damage structures to fully exploit their capability in the inelastic range. A summary of the main design parameters for both design methods and building technologies can be found in Appendix-Table 6.

Considering all the building configurations (27) and the different ductility/behavior factor discretization (~10 ductility for both wall and frame direction for each building configuration), ~270 alternative moment resisting frames and structural walls are designed, for a total of 540 parametrizations. By comparing the results in terms of base shear for all the configurations analysed (Fig. 9), important considerations can be drawn. Focusing on the

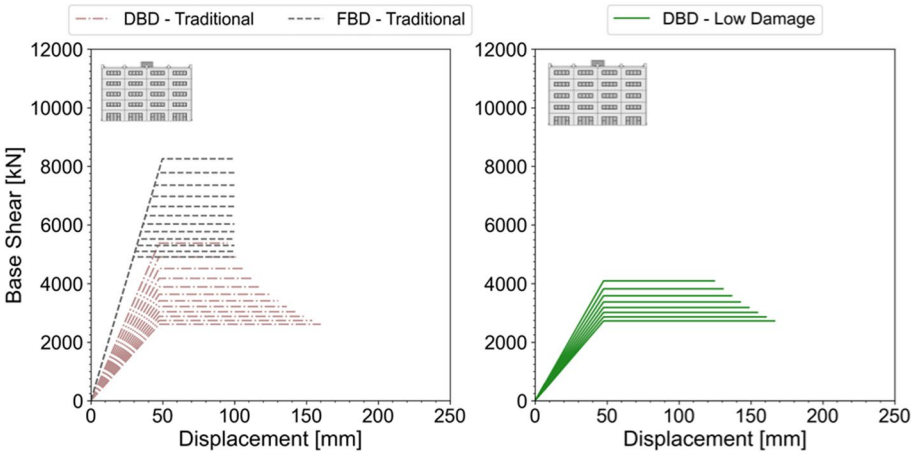

Fig. 8 Analytical capacity curves for the Traditional buildings (left) designed following FBD and DDBD procedures, and for the Low Damage buildings (right), in case of high seismicity and Importance Class II—frame direction only

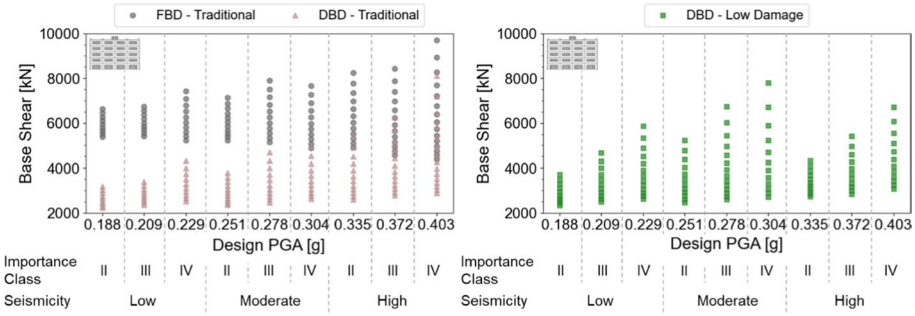

Fig. 9 Base shear vs. design PGA for the Traditional buildings (left), designed following FBD and DDBD procedures, and the Low Damage buildings (right), for frame direction only

traditional structures, it can be noticed that, due to the comparative assumptions herein adopted (see below further comments), the FBD always overestimates the building base shear for all the different design PGAs, describing the seismic intensity levels involved, when compared to the DDBD results. Yet, the latter are assumed to provide a more reliable ("correct") structural response. The difference between the two methods is more evident in the wall direction where the base shear demand is greatly overestimate. In many cases, the higher value of base shear brings to an increase of the sectional dimensions of concrete beams and columns. This is caused by the excessive demand on the structural elements, thus creating a unnecessary overstrength to the building. It is worth mentioning that, due to the assumption of same ductility level for the two alternative design methodologies (FBD and DDBD), reasonable behaviour factors ($q < 4$) are considered in this study, which would not necessary be the case in the design practice where higher values of q up to the maximum allowed in the code (e.g. $q = 5.8$ for multi-story multi-span frame structures, according to the Italian code) would/could be adopted leading to lower base shear values. When considering the hybrid low damage structural skeleton, a slightly higher base shear is obtained when compared to the traditional solution with same ductility level, due to the lower hysteretic damping value. This is due to the resisting moment capacity, which is distributed between dissipative and recentering systems, consequently leading to lower dissipation when compared to the case of monolithic connections.

3.2 Design of structural connections

An equilibrium approach is employed to distribute the base shear throughout the structural system, in order to obtain the internal actions in the structural connections (beam-column joints, column-foundation, wall-foundation). Section analysis is developed to design the steel reinforcement and compute the moment-rotation/curvature relationships of all the structural members. Traditional buildings are designed to exhibit a beam-sidesway mechanism (by applying a column-to-beam strength ratio of 1.3), thus neglecting shear failure as per hierarchy of strength principles. Therefore, a pure flexural plastic hinge mechanism is considered at both ends of the RC seismic beams, while for the vertical elements, i.e. RC seismic columns and walls, an axial-flexural interaction is introduced. Furthermore, two limit states are taken into account for the monolithic seismic connections: (1) the yielding

of the steel reinforcement and (2) the achievement of the concrete ultimate strain in the external fiber of the section.

Moment-rotation relationships are also obtained for the low-damage hybrid connections following the procedure described in Pampanin et al. (2010), i.e. considering the moment-resisting contribution of both post-tensioning cables/bars and external *Plug&Play* dissipaters. In the vertical members the axial load also contributes to the re-centering capability of the system, thus this contribution is embedded in the calculations. For the hybrid connections two different limit states are identified: (1) collapse of the external dissipaters and (2) yielding of the post-tensioned cables/bars (for the seismic beams and rocking walls only; concrete columns are not designed as post-tensioned elements). The number of dissipaters and their features (e.g. fuse length and diameter) as well as the number of cables/bars and their initial post-tensioning forces are optimized to achieve a moment capacity at the design drift perfectly equal to the seismic demand (Capacity = Demand). This is possible due to the design flexibility of these connections and their non-standardization, thus allowing for the selection of ad-hoc key parameters. Conversely, traditional components are less easy to optimize since steel rebars have standard diameters and, following the good practice, no more than two different diameters are usually considered within the same member. Nevertheless, an optimization is performed considering these boundary conditions (fixed diameters and maximum two different values), to find out the best combination of diameter values and number of steel bars which would reduce as much as possible the difference between the capacity and the demand.

Figure 10 shows the difference between the two technologies in terms of connections design. As previously discussed, construction limitations do not allow traditional connections to perfectly match the design requirements in terms of bending moment and

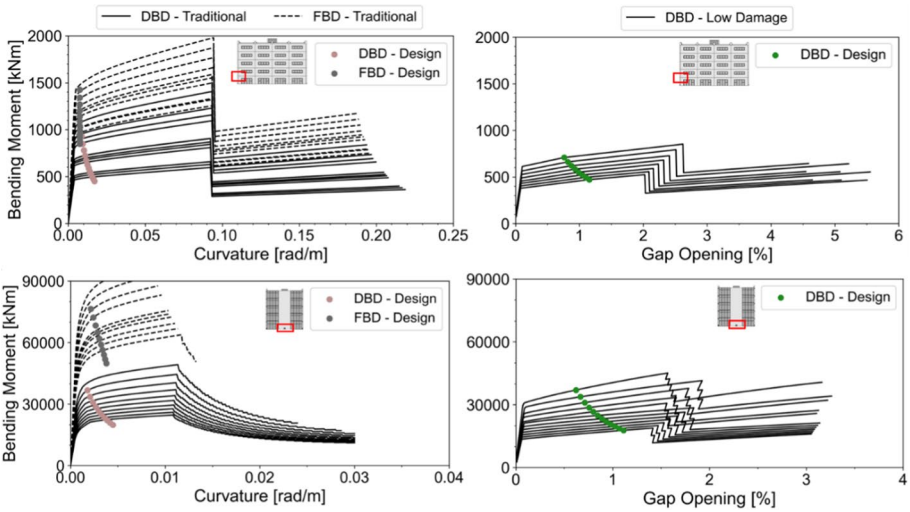

Fig. 10 Moment–curvature/rotation relationships of seismic beams (first floor) and structural walls for both Traditional buildings (left) and Low Damage buildings (right), for the case of high seismicity and Importance Class II

curvature, while hybrid connections provide the same bending moment and gap opening as per design values. Furthermore, once the dissipaters reach the ultimate strain value (set at 6%) the hybrid connections still have moment-resisting capability due to the post-tensioning cable/bars. It is also noticed that the structural walls designed according to the FBD procedure are characterized by a brittle failure mode due to the achievement of the concrete ultimate strain in the external fibers happening before the failure of the steel reinforcement.

3.3 Numerical investigation

Numerical non-linear static (push-over) analyses are performed for all the case studies through Ruaumoko2D software (Carr 2003). It is worth mentioning that, given that the building is perfectly symmetrical in both directions and a rigid diaphragm is adopted at each floor, a 2D model can be adopted to decouple the building behavior in the two orthogonal directions. If this assumption was not valid, a 3D model is suggested to properly capture the possible torsional effects and out-of-plane behaviour. A lumped plasticity approach is adopted to describe the nodal regions where the inelastic behaviour is expected. Rigid zones are assumed in the beam-column joints and the structural elements are modelled as elastic members linked together through springs, described by the moment-rotation relationships computed in the section analysis and using proper hysteresis rules. For the monolithic frame (Fig. 11-left), the springs represent the plastic hinge regions (Takeda hysteresis) designed to develop a beam-sidesway mechanism, while the columns also account for the moment-axial force interaction through the definition of their yield interaction surface. In the wall direction, the plasticity is concentrated at the base connection of the structural wall, while the rest of the component is assumed elastic. For the low-damage structure (Fig. 11-right) two rotational springs are introduced at the end sections of the structural members—beam-column joints, column base and wall base—(Pampanin et al. 2001) to simulate the combined action of energy dissipation (Ramberg–Osgood hysteresis) and re-centering (multi-linear elastic). Stiffness degradation in the structural connections is neglected, as well as the soil-structure interaction (fixed connections are assumed at the base sections). Moreover, second order effects are not taken into account in the analysis.

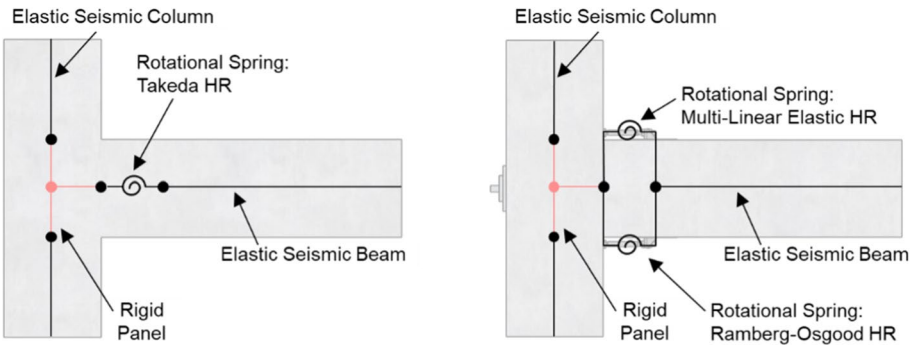

Fig. 11 Schematic representation of the lumped plasticity modelling approach adopted for the traditional (left) and low-damage (right) connections

Through a non-linear static approach, numerical pushover curves are obtained and compared with the analytical design values. The design point is identified on the numerical curves by the achievement of the design curvature/rotation demand at section level. Specifically, for the moment-resisting frame system the average of all the curvature/rotation values is considered, while for the structural wall the curvature/rotation of the plastic hinge at the base is considered. By comparing the analytical design displacement and base shear with the numerical pushover curves different findings can be discussed. Overall, the DDBD procedure presents lower difference in terms of building strength and displacement at the design point for both frame and wall structural systems when compared to the building designed following the FBD procedure. Particularly, differences are greater considering the wall direction due to the larger seismic demand produced by this method. Moreover, the initial stiffness is well captured using the DDBD procedure, except for the low-damage structural walls. In this case, the analytical procedure underestimates the elastic stiffness due to the presence of post-tensioned bars in the walls, which increase the initial elastic contribution.

Afterwards, non-linear push-over curves are converted into acceleration-displacement curves in the Acceleration Displacement Response Spectra (ADRS) domain. In the same graph, the demand spectra of nine different seismic intensity levels, representing the

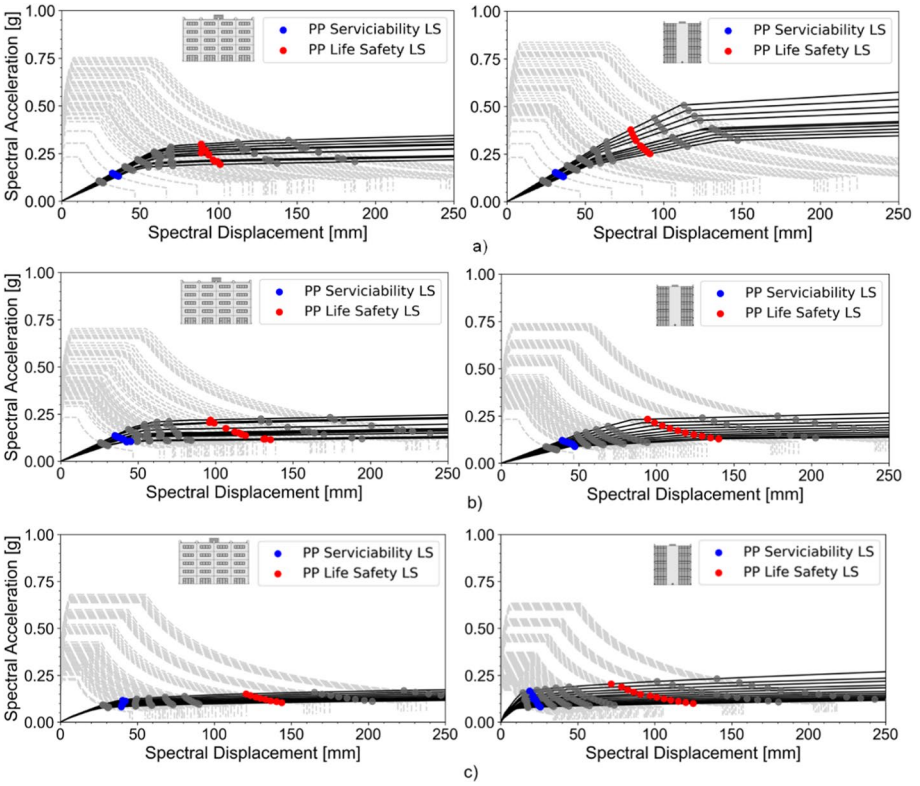

Fig. 12 Acceleration Displacement Response Spectra (ADRS) domain for frame (left) and wall (right) directions considering a) FBD—Traditional, b) DDBD—Traditional and c) DDBD—Low Damage buildings, for the case of high seismicity and Importance Class II

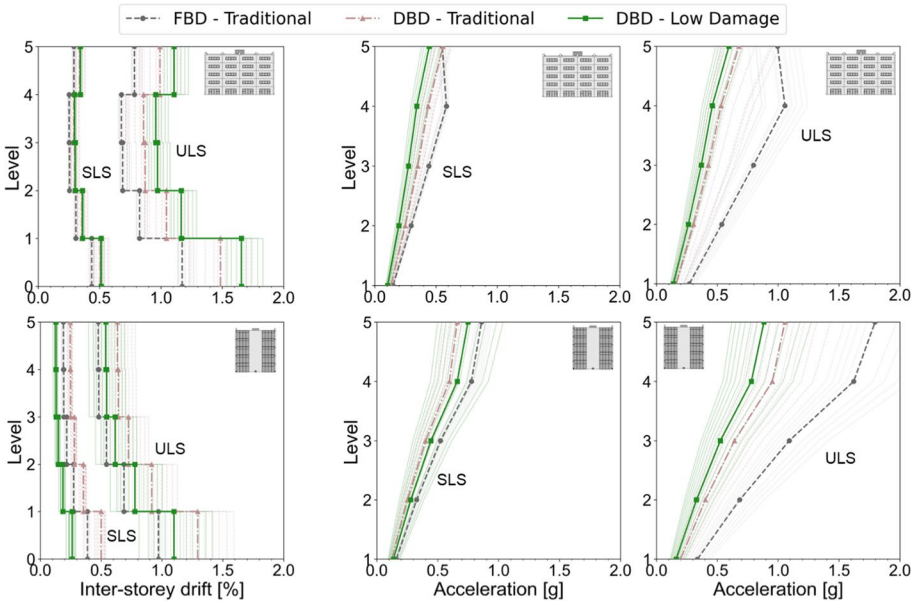

Fig. 13 EDPs average values in terms of interstorey drift ratio (left) and floor accelerations (centre, right) for both Traditional and Low Damage buildings in both frame (top) and wall (bottom) directions, for the case of high seismicity and Importance Class II

following probability of exceedance: 81%, 63%, 50%, 39%, 30%, 22%, 10%, 5%, 2%, from Frequent Earthquake to Maximum Probable Earthquake, are also included. These demand response spectra are obtained from the elastic response spectra using the η reduction factor supported by Priestley et al. (2007), in turn defined by the equivalent viscous damping of the building. Applying the Capacity Spectrum Method (ATC 40 1996), the Performance Points, representing the maximum expected seismic displacements and accelerations, are obtained for of all the case-study configurations at each seismic intensity level (Fig. 12).

All the graphs in Fig. 11 show that the PRESSS technology allows to move the performance points of the building towards higher displacements, especially at the ultimate limit states (ULS) and for the frame direction. This is simply due to the low-damage structures accounting for less dissipative capability and therefore higher spectral reduction factors ($\eta_{Trad} < \eta_{LD}$).

To develop the seismic loss evaluation, inter-storey drifts and floor accelerations (Engineering Demand Parameters, EDP) are calculated from the performance points identified in the ADRS domain. The floor displacements are derived referring to the displacement shape of the buildings, while the floor accelerations are obtained accounting for the base shear along the height of the building and using the floor masses. The accelerations and displacements values are then corrected by considering proper factors to account for the high mode effects (FEMA P-58–1 2018). Figure 13 shows the EDPs for the Serviceability limit state (SLS, 63% probability of exceedance)

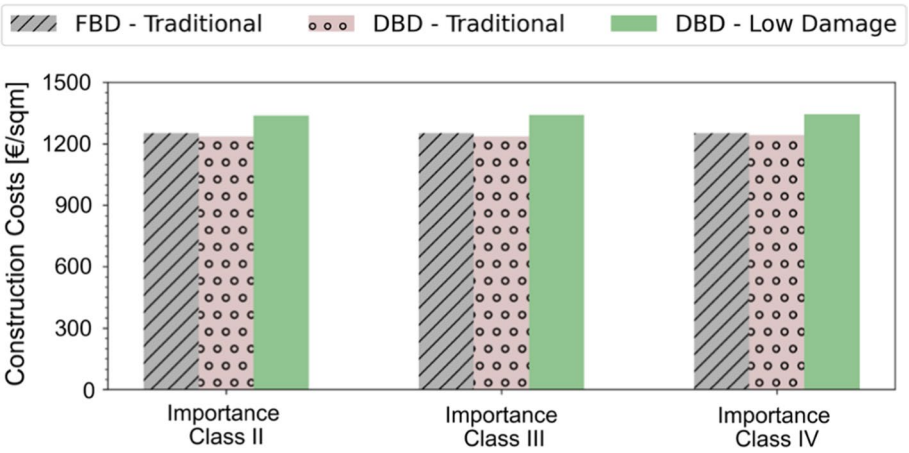

Fig. 14 Construction costs (average) for high seismicity and different Importance Classes

Table 2 Average values of construction costs for all the building configurations

	Construction costs								
	Low seismicity			Moderate seismicity			High seismicity		
Importance class	II	III	IV	II	III	IV	II	III	IV
FBD—Trad. [€/m^2]	1251.0	1251.4	1251.6	1254.0	1258.1	1258.1	1253.4	1254.0	1255.1
DDBD—Trad. [€/m^2]	1237.3	1237.5	1243.1	1238.3	1240.0	1244.1	1241.8	1247.3	1250.0
DDBD—LD [€/m^2]	1337.8	1340.5	1344.9	1342.7	1348.8	1353.2	1343.3	1348.3	1355.2

and the Ultimate limit state (ULS, 10% probability of exceedance) for both frame and wall directions.

Overall, it can be observed that the inter-storey drifts are larger in the frame direction while the acceleration values are greater in the wall direction on average. Particularly, FBD procedure always produces a higher acceleration demand to the building when compared to the DDBD methodology, and DDBD usually leads to larger demand in terms of inter-storey drift, as expected from the analytical comparison. Higher acceleration/drift values will lead to higher damage in the acceleration/drift sensitive non-structural components when implementing the loss modelling analysis. It is worth highlighting that, as discussed above, the obtained results are affected by the assumption made on the q factor, used to implement the FBD approach and assumed as the same ductility value of the DDBD method. Rather, when a design practice approach is followed, the q factor is typically selected as the maximum allowed by the code provisions to achieve the lowest seismic demand. In this case, base-shear and acceleration values might be lower for the FBD when compared to the DDBD, as shown by Gentili et al. (2021). This means that the FBD method does not allow to have a proper control on the nonlinear behavior of the structure, due to its procedure based on the selection of a behavior factor (q) representing the dissipation capability of the building under consideration. Appendix-Table 7 lists the maximum EDP values within any ductility

range (min and max are referring to minimum and maximum ductility values) for all the building configurations and seismicity levels.

4 Construction costs

Construction costs are computed for each building configuration based on the "Prezziario Unico del Cratere del Centro Italia" DPCM (2018) (price list developed after the 2016 Central Italy Earthquake). The cost of the monolithic structures is calculated considering the total concrete volume and steel needed for the structural elements, as well as the cost of formworks, safety, excavation, foundations, and geotechnical surveys. For the PRESSS structures, the cost of the tendons and their post-tensioning, the corrugated tube and the crane rental are added to the above items (apart from the cost of in-situ formworks, not needed for precast elements). An additional variable cost, depending on the number of dissipaters and post-tensioning cable/bars, is taken into account for each hybrid connection, meaning the supplemental cost of all the prefabricated special steel assemblies and members. Architectural components, finishing and equipment costs are instead obtained from supplier cost lists or taken from "Prezzi per Tipologie Edilizie" DEI (2012) referring to the average cost of a 7-storey RC residential building in Italy.

A comparison in terms of average construction cost for the alternative case-study configurations is provided in Fig. 14 and Table 2. It can be noticed that the FBD provides costs equal to, or slightly higher than, the DDBD for the same seismicity zone, on average. Moreover, as far as a comparison between technologies is concerned, it can be noticed an increase of construction costs for the PRESSS technology of around 8% for low-to-high seismic intensity, when compared to the monolithic system.

Overall, the increase of direct costs associated with a significant increase of steel reinforcement, moving from Importance Class II to III and IV, is negligible when compared to the total building cost, since this study is carried out considering the same building geometry. In traditional buildings, the higher seismic demand is managed by adding supplemental steel reinforcements or considering larger bar diameters (still respecting the good practice and code requirements), while, in case of low damage structures, by sizing the dissipaters and considering an increase of the initial post-tensioning force in the structural members. This consequently leads to negligible differences when an increase of seismic demand at same seismicity level is considered, thus supporting the hypothesis that rising the bar in seismic design require much less additional costs than expected. Arguably, a significant level of higher safety for new constructions could and should be achieved with minimal investment.

5 Fragility specification

The loss modelling implementation, following the probabilistic Performance-Based Earthquake Engineering methodology (Cornell et al. 2002; Krawinkler and Miranda 2004; Gunay and Mosalam 2013), involves the identification of potential damage state levels (fragility curves) and related repair costs and time (consequence functions). Fragility specifications for traditional components, including structural and non-structural elements, are defined by FEMA P-58–1 (2018) fragility database, while equivalent fragility data needed to be computed for the low-damage components, i.e. the hybrid connections: beam-column joints, wall-foundation and column-base.

Fragility curves for the hybrid connections are determined from the analytical section analysis (moment-rotation relationship) assuming two limit states: (1) collapse of

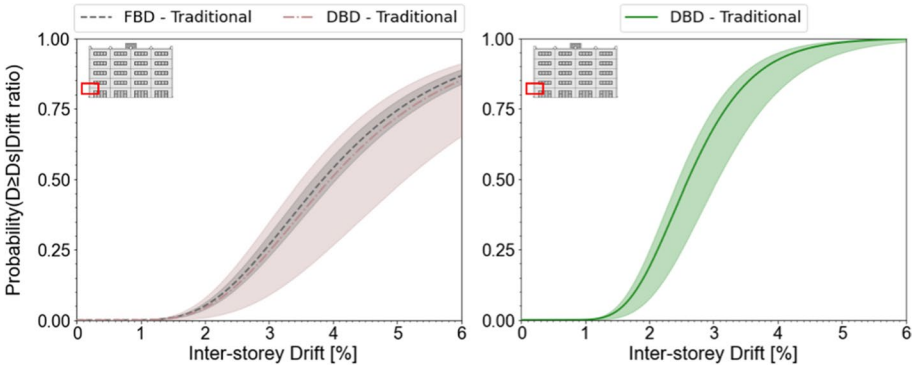

Fig. 15 Comparison in terms of fragility curves for monolithic (DS2, left) and hybrid connections (DS1, right) for a beam-column joint at the first floor, for the case of high seismicity and Importance Class II

the external dissipaters (DS1) and (2) yielding of the post-tensioned cables/bars (DS2). Due to the reliable numerical modelling approach, extensively calibrated and validated through experimental tests (e.g. Pampanin et al. 2001; Johnston et al. 2014; Ciurlanti et al. 2022), numerical rotations on each connection, associated with the analytical gap openings, are identified on the pushover curves and consequently inter-storey drifts are obtained corresponding to that damage state. Dispersion value of the fragility curves is assumed equal to 0.3, considering that these connections exhibit a better and controllable behavior. Although the damage states for the traditional connections can be derived from FEMA database (residual crack widths > 0.06 inches for DS1, initial spalling of cover concrete for DS2, possibility of having core concrete crushing, fracture or buckling of reinforcement for DS3), following the same approach previously described, a section analysis is carried out to identify both DS2 and DS3.

Figure 15 shows a comparison between low-damage and traditional components for both frame and wall directions in terms of fragility curves (DS2 for the monolithic connections vs. DS1 for the hybrid connections). Results highlight that the wall connections designed using the FBD procedure show higher probability of exceeding the DS2 damage state when compared to the wall connections design by DDBD at same drift level. For the frame connections, this consideration is still valid when exploiting the full range of ductility (Fig. 15 left). Moreover, it can be observed that the first damage state (DS1) associated with low damage members (Fig. 15 right) is achieved at higher seismic demand levels when compared to the second damage state (DS2) of traditional connections. This further confirm that a low damage structure could help to enhance the seismic safety of the building.

The consequence functions are instead built referring to the data available in the FEMA database, i.e. the DS2 of the hybrid connections (yielding of post-tensioned cables/bars) is conservatively assumed equal to the DS3 of the monolithic connections, while the repair cost and time of DS1 (collapse of the external dissipater) are estimated based on market prices and engineering judgment (i.e. 1000€ for beam-column joints and 1500€ for the wall-base foundation).

6 Loss assessment analysis

Post-earthquake losses estimation is crucial to evaluate the convenience of a design strategy during the life-span of a building. The economic aspect is fundamental within the conceptual design stage of a building project, and represents the main factor driving the choice of a technological solution. Proving that a safer solution is also the least expensive at the end of the life time of the building, is therefore essential to argue that the current traditional performance-based design approach, still targeting the life safety, is not enough to line up with advanced earthquake risk reduction policies.

The estimation of post-earthquake losses is carried out in the Python algorithm through the *pelicun* framework developed by SimCenter (Zsarnóczay and Deierlein 2020), which implements the rigorous probabilistic procedure provided by FEMA P-58–1 (2018), accounting for both direct and indirect economic losses. Once all the required information about hazard (intensity measure of the earthquake), seismic performance (through the calculated EDPs) and damage states (fragility curves) are collected as presented in the previous sections, the entire set of building configurations is analyzed by loss analysis and results are compared in terms of EAL, a key parameter for decision makers directly related with insurance policies. All the analysed frame and wall systems are thus coupled to fully explore all the possible combinations within any seismicity and Importance Class variation (~ 10 duct. Frame x ~ 10 duct. Wall = ~ 100 buildings assessed). Considering nine seismic intensity levels (from Operational limit state to more than Collapse Prevention) within any seismicity zone, Importance Class, and design methodologies/technologies involved, ~ 24,300 loss assessment are performed. This number highlights the huge potentiality of the workflow implemented to carry out this study; "black box" tools as well as tools accessible from the user interface would be inefficient due to the large number of analyses involved. By selecting a time-based assessment, the repair costs/frequency curves are thus obtained for all the building configurations, and consequently the EAL. Figure 16 presents a comparison between these curves considering high seismicity and Importance Class II. Lower and upper bounds, corresponding to the 16th and 84th percentiles, are also shown to assess the variability associated with the different ductility values.

Figure 16 highlights that generally the DDBD procedure, even better when combined with a high-performance technology, allows to drag the cost/frequency curves towards lower repair costs, while providing higher safety levels associated with the raising of the bar in seismic design. Interesting to note that, concerning the low damage structures, repair costs at higher MAF (Mean Annual Frequency), thus lower return periods earthquakes, are slightly larger when compared to traditional buildings. This is mainly due to the failure of acceleration-sensitive non-structural components in the wall direction. It is worth noting that all the buildings configurations assessed in the parametric study involve the same non-structural configuration, while, in case of low damage buildings, non-structural elements need to and can be protected from the expected slightly larger drifts for frame systems and higher accelerations in the structural rocking wall systems, depending on the selected ductility/drift design value.

EAL values can be easily computed as the area under the curves of all the case studies. Building 3D EAL surfaces (e.g. for high seismicity and Importance Class II in Fig. 17) as a function of the variability associated with the design ductility, it can be observed that FBD methodology, in spite of leading to larger base shear and thus apparently higher protection, always produces higher seismic losses when compared to

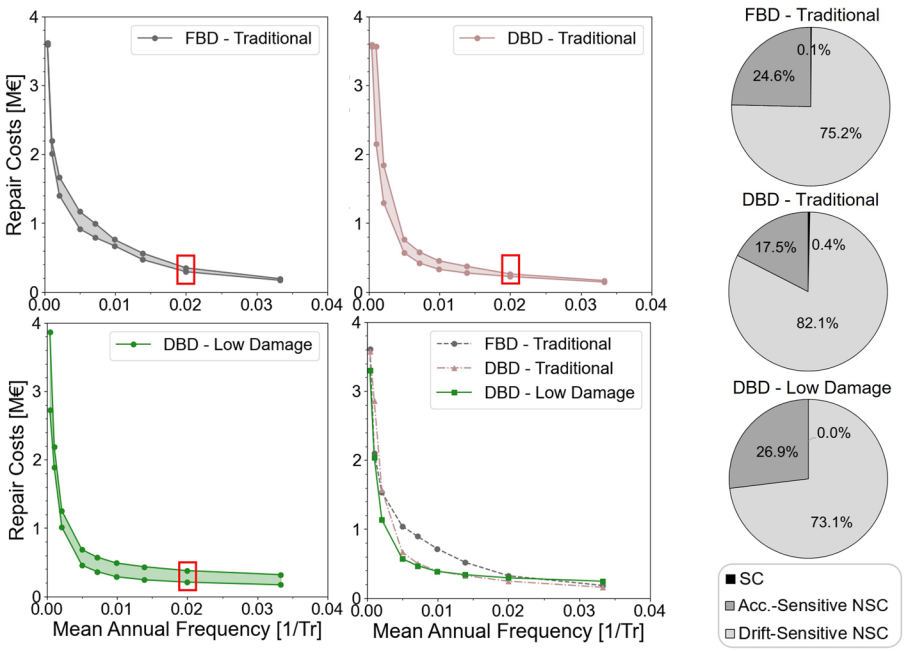

Fig. 16 Comparison in terms of EAL curves for high seismicity and Importance Class II considering lower and upper bounds referring to 16th and 84th percentiles and average curves. Percentage of losses for Structural Components (SC) and Drift -and Acceleration- sensitive Non-Structural Components (NSC) for a low-seismic intensity (Serviceability Limit State)

a methodology controlling the displacement for the full range of ductility investigated. These higher seismic losses are due to the acceleration-sensitive non-structural components, experiencing larger accelerations due to the larger base shear, as well as to the poor ductile behaviour of the structural members, characterized by a brittle failure

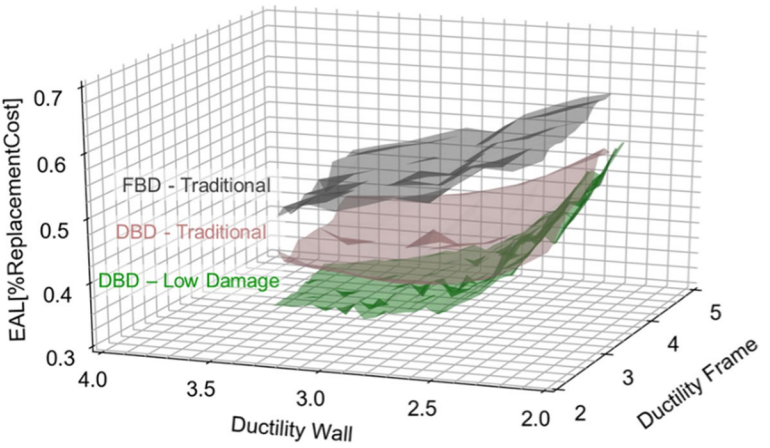

Fig. 17 3D EAL surface for the case of high seismicity and Importance Class II

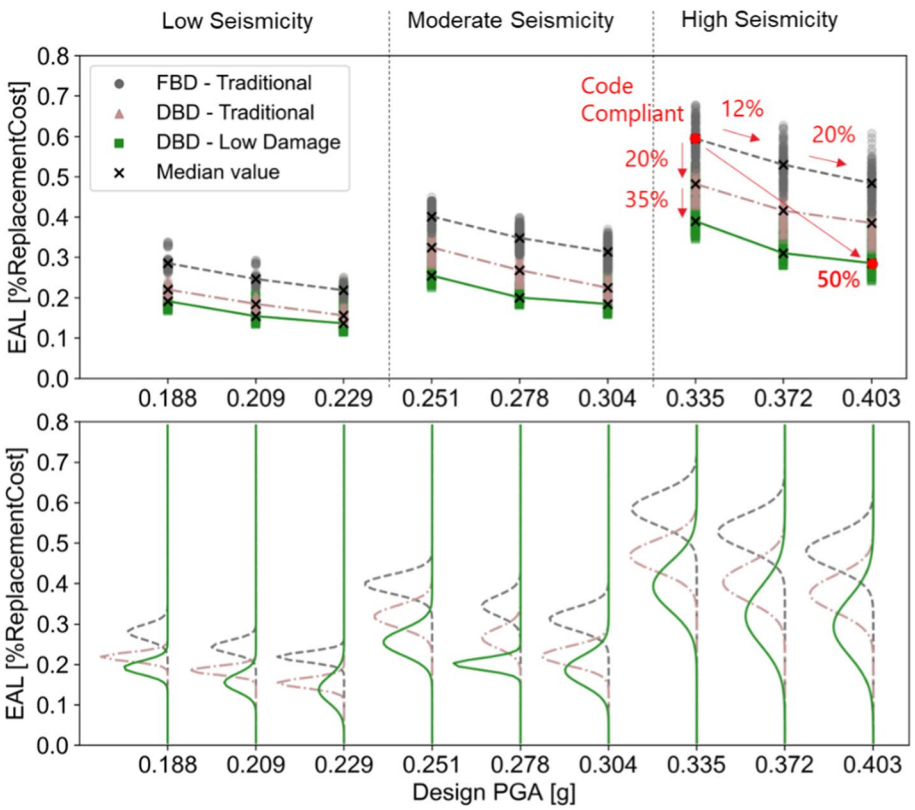

Fig. 18 Results in terms of EALs for all the building configurations

mode thus producing higher damage and associated repair costs when the damage conditions are achieved. Furthermore, as expected, a further reduction is obtained when an advanced design methodology is used in combination with an innovative technology.

Finally, the overall results in terms of EAL are presented in Fig. 18 and herein discussed. All the observations made previously are still valid for the other seismicity levels and Importance Classes. Assessing and comparing all the building configurations, results highlight that:

1. when referring to the average value, as the Importance Class increases, the seismic losses decrease, due to the increased level of safety thus consequently leading to reduced seismic losses. This outcome is observed for all the seismicity investigated, proving that increasing the seismic demand brings to less seismic losses without significantly increasing the construction costs.
2. comparing the results obtained for the same construction technology whilst varying the design method, FBD produces greater losses than the DDBD, confirming the actual disadvantage of applying such traditional design methodology, although being considered as a more "conservative" and thus "safe" approach.

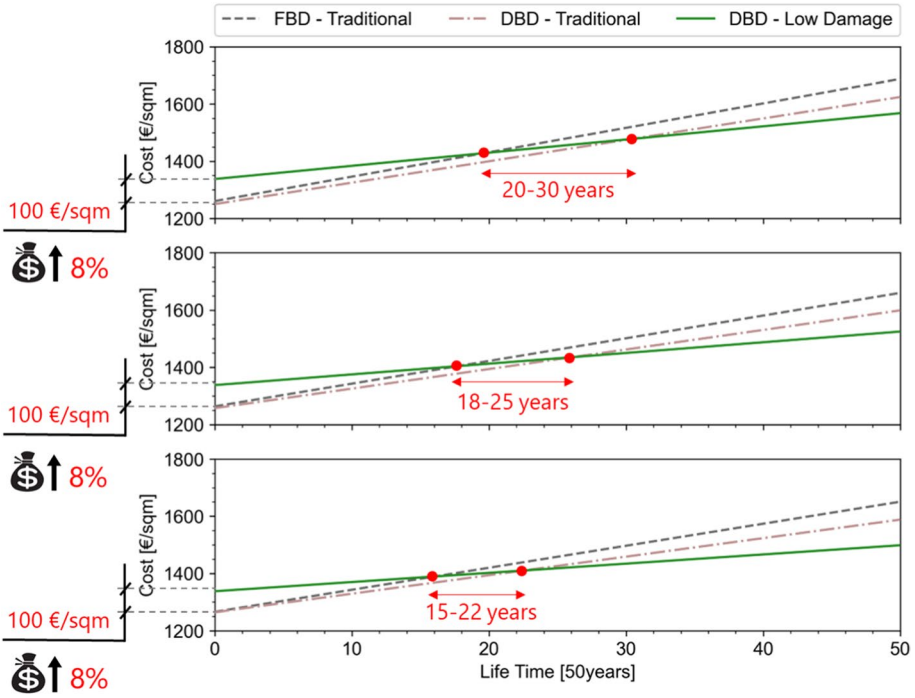

Fig. 19 Cost/time curves (average values) in case of high seismicity and different Importance Classes

3. looking at the different types of skeleton systems, PRESSS structures lead to significantly lower losses when compared to monolithic structures, due to its inherent low-damage nature.

Concerning the dispersions associated with the variation of the design ductility, low damage structures generally present a larger variability when compared to traditional solutions. As previously discussed, combinations considering stiffer structural walls (designed for low ductility values) bring to larger seismic losses which affect the acceleration-sensitive non-structural performance. The latter could be easily solved by employing low-damage solutions for non-structural elements, e.g. by introducing simple modifications detailing to suspended ceilings (e.g. the use of elastic insulation foam as described in Pourali et al. 2017). On the other hand, low-damage structures could be designed to fully exploit their non-linear behavior, thus considering larger ductility values (which have not been explored in this specific investigations).

6.1 Seismic costs in the building life

Finally, the seismic costs of all the case-studies are compared at the end of the service life (e.g. 50 years after the building construction) to better appreciate the benefits of applying advanced seismic design methodologies and technologies. This comparison can be carried out in terms of annualized losses (the EAL parameter) distributed along 50 years in

Table 3 Comparison in terms of savings at the end of the building service life (50 years)

	Costs at the end of the building life								
	Low seismicity			Moderate seismicity			High seismicity		
Importance class	II	III	IV	II	III	IV	II	III	IV
FBD—Trad. [€/m^2]	1466	1438	1414	1544	1516	1492	1687	1660	1651
DDBD—Trad. [€/m^2]	1398	1371	1368	1495	1461	1444	1624	1599	1588
DDBD—LD [€/m^2]	1446	1425	1412	1486	1457	1443	1568	1525	1499

order to evaluate the percentage of construction cost which would be lost at the end of the building life. The cumulative seismic cost is described by a linear trend going from the initial cost at the time of construction to the cost at the end of the building service life. No economic fluctuation is considered in this model. The intersection between the different lines, representing different design strategies, identify a virtual break-even time at which the initial difference in the initial construction costs would be balanced (investment return period). Although the PRESSS technology requires a slightly higher investment than the traditional system, the trend is completely reversed from the year corresponding to the intersection of their cost lines onward. This is shown in Fig. 19 for e.g. high seismicity zone. The difference in the initial cost of around 8% (low-damage vs. monolithic, with traditional non-structural components) at the time of construction is fully recovered in a range between 20 and 30 years (for Importance Class II) when compared to the FBD and DDBD traditional buildings, respectively. Another important observation is that the investment return period decreases moving towards higher Importance Classes (III and IV), i.e. reducing by around 15 years when compared to a code-compliant (FBD) traditional building, without affecting the initial construction costs. This means that designing the building to withstand a higher seismic demand, e.g. targeting the building to be of the same importance class typical for hospitals or strategic structures, meaning higher structural safety, does not (or only slightly) affect the initial investment, but drastically reduce the seismic losses and the investment return period. This provides an additional and strong evidence/confirmation that it is definitely worth considering advanced methodologies and technologies to mitigate the seismic risk and therefore the impact of earthquakes on the community.

A summary of the average savings after 50 years from the time of construction, for each seismicity area and importance class, are shown and compared in Table 3. The savings are clearly more consistent in high seismicity areas and, consequently, the benefits of implementing low-damage technology are more evident.

7 Application of a logistic prediction model

The implemented parametric study highlights the variability in terms of performance and cost depending on the design ductility value selected within any seismicity/importance class investigated. Specifically, each pair made by a frame and wall ductility value leads to different building performance (backbone curve) and consequently seismic losses, building up a direct relationship between the expected EAL and the design inter-storey drift (or ductility, in turns related to the selected design inter-storey drift) of the building. Therefore,

Table 4 Beta coefficients of the logistic regression models

	Beta coefficient		
	β_0	Frame—β_1	Wall—β_2
DDBD—traditional	0.64	−3.28	2.51
DDBD—low damage	7.647	−0.913	6.110

for a given seismicity level (e.g. high seismicity), importance class (e.g. Importance Class II) and technology (traditional or low damage), a basic machine learning technique is employed to identify the best design ductility range where the EAL value is less than 0.5%. This value represents the upper threshold to collocate the building in the lowest Italian risk class A^+ (DM 58 2017).

To develop this study, a logistic regression model is implemented in order to predict the ductility level for which the building has more than 90% chance to be under the EAL threshold value. This prediction model allows to manage binary classification problems and is based on a Logistic function from where the name comes from. The Logistic function or Sigmoid function is a S-shaped curve where Predictors (or Input values, x_i) are combined linearly using weights β_i to predict an output binary response variable in probabilistic terms (p):

$$p = S\left(\beta_0 + \Sigma\beta_i x_i\right) \tag{5}$$

In order to create a larger data, 1000 ductility values for both frame and wall direction are selected considering all the case studies (FBD—Traditional, DDBD -Traditional, and DDBD—Low Damage) for high seismicity and importance class II. Hence, by combining all those cases, 1 M loss assessments are identified for each building configuration. Then, results in terms of EAL are converted into a binary value equal to 1 for EAL < 0.5% and equal to 0 for EAL > 0.5%. Two Predictors are selected, namely: (1) design ductility values referring to the frame (x_1) and (2) wall direction (x_2). Concerning the beta coefficients, they are estimated using the maximum likelihood-method, thus minimizing the error between the predicted model (based on those coefficients) and the training data set (assumed as the 30% of the entire data set). Table 4 lists the β coefficient values for both frame (β_1) and wall direction (β_2), while β_0 is the intercept. The case studies designed using FBD method

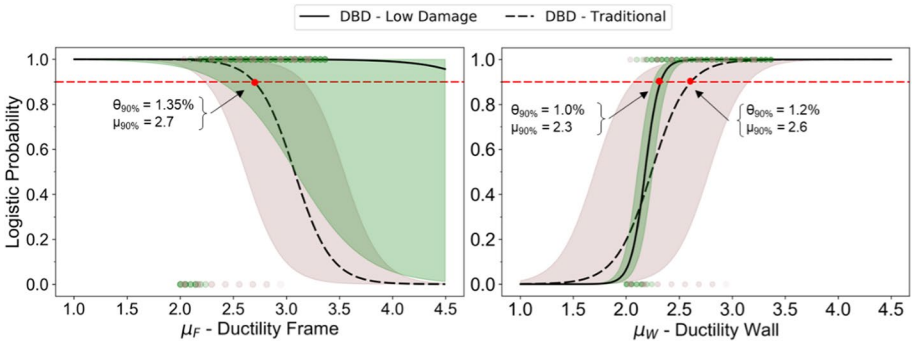

Fig. 20 Logistic functions and their confidence intervals for frame (left) and wall (right) directions

presents few EAL values under the threshold of 0.5%, thus FBD is excluded from this specific study due to the unbalanced data set.

First, two opposite signs (negative/positive) can be observed for frame and wall direction, specifically a negative sign for the coefficient of the frame system (β_1) and a positive sign for the structural wall (β_2). This means that the higher is the values of the frame ductility, the lower is the probability to achieve an EAL less than 0.5%, while the opposite consideration can be stated for the wall direction, i.e. the higher the ductility value is, the higher the likelihood to be in a A^+ risk class is. Furthermore, the magnitude of the coefficients is also important to figure out the trend of the prediction models. It can be noticed that the contribution of both building directions is balanced for the traditional solution while the wall direction contributes more in case of low-damage system. All these observations are clearly shown in Fig. 20, where the comparison between Logistic functions is presented.

The Logistic functions (black lines) are computed by fixing one Predictor (x_i) to the median value and by varying the other within the entire range investigated (e.g. for the frame direction, the wall ductility is fixed, while the frame ductility is variable). The confidence interval is related to the 16th and 84th percentile (e.g., for the frame direction, the range represents the influence of the wall direction).

Figure 20-left shows how limiting the design drift values for moment resisting frame systems most likely leads to higher probability to achieve an EAL < 0.5% (A^+ risk class, according to DM 58 2017). Specifically, when 1.35% inter-storey drift (corresponding to a ductility of 2.7) is exceeded, the probability of achieving 0.5% EAL starts decreasing for the traditional solution. Moreover, a large variability associated with the wall direction is observed from the confidence interval in the same graph. For the wall direction (Fig. 20-right), an opposite trend is observed, i.e. designing a ductile structural wall improves the probability to locate the building in A^+ risk class. Acceleration-sensitive components, such as equipment, workstations and suspended ceilings, are in fact potentially very vulnerable in a building comprising stiffer structural walls. Therefore, to reduce the probability to achieve higher seismic losses, structural walls need to be designed between 1.2 and 1.5% of inter-storey drift ratio. Finally, the irrelevant contribution of the frame direction for the low damage structures is also observed, still reflecting the high performance of the system.

8 Conclusions

This study has focused on the cost/performance evaluation and comparison of alternative design strategies which might be adopted to enhance the seismic safety of new buildings. By considering increasingly levels of seismic intensity (representing either a higher seismicity zone or a higher Importance Class), different design methodologies (Force-Based Design vs. Displacement-Based Design) or technologies (Traditional vs. Low Damage) are implemented to develop the proposed parametric study.

Results allow for a greater awareness of the proper design strategy to be used for new buildings and the main research findings are herein summarized:

- Force-based design brings to different results (yet not necessarily conservative) when compared to the displacement-based design. The parametric study on alternative structural configurations has indeed highlighted that the building response in terms of base shear is usually overestimated. However, this does not mean that the FBD is a more conservative method than the DDBD approach (as it could in turn underestimate the

displacement-ductility demand), but rather it proves that this approach does not allow to have a proper control of the real structural behaviour, and in general on the seismic results.

- The parametric study shows that the base-shear, that is a fundamental parameter for the seismic design since it allows to determine the demand moment/shear values in the structural members, does not necessary nor directly increase with the assumed level of seismic intensity, expressed in terms of Peak Ground Acceleration (PGA). Therefore, designing for higher Importance Classes, meaning a greater safety and resilience, does not necessarily lead to an proportionally increase in costs. Instead, minor but appropriately focused investments can lead to greater safety, resilience and long-term savings.
- Taking into account the initial construction costs and focusing on high seismicity area, it can be observed that when moving from Importance Class II to IV, although the base shear is higher, a negligible difference is observed in the total investment. Furthermore, the advantage related to the implementation of a low-damage technology such as the rocking-dissipative PRESSS system is evident, especially for the case-studies where post-earthquake damage causes very high repair costs (high seismicity).
- When considering the cumulative seismic cost over time, the convenience of designing through a displacement-based approach is evident (overall long-term seismic costs are always lower when compared to FBD). When low-damage technologies are adopted, the initial higher cost (around 8%) is fully recovered in less than 15–20 years and a reduction of EAL of around 30%-50% is obtained when compared to the traditional systems. Therefore, investing in innovative solutions is always convenient.
- The computed savings at 50 years (service life) after the time of construction show that the greatest savings for the low-damage technology refer to Importance Class IV and high seismicity zone. However, this consideration does not lead to the conclusion that in areas with a low seismicity, low-damage connections are not convenient; savings are obtained for all seismic-prone areas and Importance Classes, so it is clear that designing better, that means for better performance and greater safety, is always also (socio-) economically convenient and leads to a more resilient community.

This paper has therefore developed a comprehensive parametric study to compare the cost/performance of different case-study buildings with different design parameters, design methods, and/or construction technologies, to highlight the actual and significant economic benefits associated with a significantly reduced level of damage, and thus limited post-earthquake economic losses (rarely addressed/computed in literature). Although important findings have emerged from this parametric study, further investigations are needed to compare the alternative design methods and technologies and to prove the convenience of implementing enhanced-safety design strategies. Future research will particularly focus on the development of fragility analyses, needed to determine the reliability of the alternative design procedures, i.e. looking at the influence of the design approach on the building probability of collapse.

Appendix

See Tables 5, 6 and 7

Table 5 Building configurations considered for the investigation

	FBD—Traditional								
	Low seismicity			Moderate seismicity			High seismicity		
Importance class	II	III	IV	II	III	IV	II	III	IV
H beam [m]	0.75	0.75	0.80	0.75	0.75	0.80	0.75	0.80	0.80
B beam [m]	0.4	0.4	0.45	0.4	0.4	0.45	0.4	0.45	0.45
H column [m]	0.75	0.75	0.80	0.75	0.75	0.80	0.75	0.80	0.80
B column [m]	0.4	0.4	0.45	0.4	0.4	0.45	0.4	0.45	0.45
H wall [m]	6	6	6	6	6	6	6	6	6
B wall [m]	0.4	0.4	0.4	0.4	0.4	0.4	0.4	0.4	0.4
a_g [g]	0.125	0.125	0.125	0.175	0.175	0.175	0.25	0.25	0.25
μ_{min}—Frame	1.5	1.75	1.75	1.75	1.75	2	2	2.25	2.25
μ_{min}—Wall	1.5	1.75	1.75	1.75	1.75	1.75	2	2	2
	DDBD—Traditional								
	Low seismicity			Moderate seismicity			High seismicity		
Importance class	II	III	IV	II	III	IV	II	III	IV
H beam [m]	0.75	0.75	0.80	0.75	0.75	0.80	0.75	0.80	0.80
B beam [m]	0.4	0.4	0.45	0.4	0.4	0.45	0.4	0.45	0.45
H column [m]	0.75	0.75	0.80	0.75	0.75	0.80	0.75	0.80	0.80
B column [m]	0.4	0.4	0.45	0.4	0.4	0.45	0.4	0.45	0.45
H wall [m]	6	6	6	6	6	6	6	6	6
B wall [m]	0.4	0.4	0.4	0.4	0.4	0.4	0.4	0.4	0.4
ag [g]	0.125	0.125	0.125	0.175	0.175	0.175	0.25	0.25	0.25
μ_{min}—Frame	1.5	1.75	1.75	1.75	1.75	2	2	2.25	2.25
θ_{max}—Frame	2%	2%	2%	2%	2%	2%	2%	2%	2%
μ_{min}—Wall	1.5	1.75	1.75	1.75	1.75	1.75	2	2	2
θ_{max}—Wall	1.2%	1.2%	1.2%	1.2%	1.2%	1.2%	1.2%	1.2%	1.2%
	DDBD—low damage								
	Low seismicity			Moderate seismicity			High seismicity		
Importance class	II	III	IV	II	III	IV	II	III	IV
H beam [m]	0.75	0.75	0.75	0.75	0.75	0.75	0.75	0.75	0.75
B beam [m]	0.4	0.4	0.4	0.4	0.4	0.4	0.4	0.4	0.4
H column [m]	0.75	0.75	0.75	0.75	0.75	0.75	0.75	0.75	0.75
B column [m]	0.4	0.4	0.4	0.4	0.4	0.4	0.4	0.4	0.4
H wall [m]	6	6	6	6	6	6	6	6	6
B wall [m]	0.4	0.4	0.4	0.4	0.4	0.4	0.4	0.4	0.4
ag [g]	0.125	0.125	0.125	0.175	0.175	0.175	0.25	0.25	0.25
μ_{min}—Frame	1.5	1.5	1.5	1.5	1.5	1.5	2.5	2.5	2.5
θ_{max}—Frame	2%	2%	2%	2%	2%	2%	2%	2%	2%
μ_{min}—Wall	1.5	1.5	1.5	1.5	1.5	1.5	2	2	2
θ_{max}—Wall	1.5%	1.5%	1.5%	1.5%	1.5%	1.5%	1.5%	1.5%	1.5%

Table 6 Design key parameters for both technologies, structural typologies, design methods and all the seismicity levels considered

		FBD–traditional								
		Low seismicity			Moderate seismicity			High seismicity		
Importance class		II	III	IV	II	III	IV	II	III	IV
Frame	min b. shear [kN]	5375	5406	5227	5230	5154	4889	4913	4557	4372
	max b. shear [kN]	6621	6740	7412	7119	7906	7674	8256	8439	9697
	min duct., $\mu_{d,min}$	1.5	1.7	1.8	1.7	1.8	2.1	2.0	2.3	2.2
	max duct., $\mu_{d,max}$	1.9	2.1	2.5	2.4	2.7	3.3	3.4	4.2	4.9
	T_1 [s]	0.68	0.68	0.68	0.68	0.68	0.68	0.68	0.68	0.68
Wall	min b. shear [kN]	7295	7306	7438	7342	7217	7224	7394	8666	9282
	max b. shear [kN]	8887	8988	10,248	10,286	10,943	11,743	11,332	12,973	13,749
	min ducti., $\mu_{d,min}$	1.5	1.7	1.7	1.7	1.8	1.9	2.0	2.0	2.0
	max duct., $\mu_{d,max}$	1.9	2.2	2.4	2.4	2.8	3.1	3.2	3.2	3.2
	T_1 [s]	0.46	0.46	0.46	0.46	0.46	0.46	0.46	0.46	0.46
		DDBD—Traditional								
		Low seismicity			Moderate seismicity			High seismicity		
Importance class		II	III	IV	II	III	IV	II	III	IV
Frame	min drift, θd,min [%]	0.6	0.7	0.7	0.7	0.8	0.8	0.9	0.9	0.9
	max drift, θd,max [%]	0.8	0.9	1.0	1.0	1.2	1.3	1.4	1.7	2.0
	min duct., μd,min	1.5	1.7	1.8	1.7	1.8	2.1	2.0	2.3	2.2
	max duct., μd,max	1.9	2.1	2.5	2.4	2.7	3.3	3.4	4.2	4.9
	min damp., ξd,min [%]	11.2	12.4	12.8	12.7	12.8	14.3	14.0	15.1	14.8
	max damp., ξd,max [%]	13.4	14.5	15.8	15.4	16.4	17.5	17.7	18.7	19.3
	min b. shear [kN]	2218	2372	2533	2354	2477	2627	2612	2785	2885
	max b. shear [kN]	3195	3384	4317	3800	4706	4922	5382	6252	8103
Wall	min drift, θd,min [%]	0.6	0.6	0.6	0.6	0.7	0.7	0.7	0.8	0.8
	max drift, θd,max	0.7	0.8	0.9	0.9	1.0	1.2	1.2	1.2	1.2
	min duct., μd,min	1.5	1.7	1.7	1.7	1.8	1.9	2.0	2.0	2.0
	max duct., μd,max [%]	1.9	2.2	2.4	2.4	2.8	3.1	3.2	3.2	3.2
	min damp., ξd,min [%]	9.9	10.9	10.9	10.8	11.2	11.6	12.2	12.2	12.5
	max damp., ξd,max [%]	11.7	12.6	13.3	13.3	14.0	14.6	14.7	14.6	14.8
	min b. shear [kN]	2240	2404	2603	2392	2524	2705	2944	3973	4710
	max b. shear [kN]	3201	3406	4418	4070	4742	5520	5446	7147	8316

Table 6 (continued)

		DDBD–low damage								
		Low seismicity			Moderate seismicity			High seismicity		
Importance class		II	III	IV	II	III	IV	II	III	IV
Frame	min drift, $\theta_{d,min}$ [%]	0.6	0.7	0.7	0.7	0.7	0.7	1.1	1.1	1.1
	max drift, $\theta_{d,max}$ [%]	0.8	1.0	1.1	1.1	1.2	1.4	1.5	1.8	1.9
	min duct., $\mu_{d,min}$	1.5	1.5	1.5	1.5	1.5	1.5	2.5	2.5	2.5
	max duct., $\mu_{d,max}$	2.0	2.2	2.5	2.5	2.8	3.2	3.5	4.1	4.5
	min damp., $\xi_{d,min}$ [%]	9.5	9.6	9.6	9.9	9.8	10.1	13.9	14.1	14.0
	max damp., $\xi_{d,max}$ [%]	11.9	13.0	13.8	13.8	14.7	15.6	16.2	17.2	17.7
	min b. shear [kN]	2333	2494	2630	2481	2603	2713	2726	2844	3074
	max b. shear [kN]	3705	4674	5857	5224	6722	7796	4326	5398	6719
Wall	min drift, $\theta_{d,min}$ [%]	0.6	0.6	0.6	0.6	0.6	0.6	0.7	0.8	0.8
	max drift, $\theta_{d,max}$	0.7	0.8	0.9	0.9	1.0	1.1	1.2	1.5	1.5
	min duct., $\mu_{d,min}$	1.5	1.5	1.5	1.5	1.5	1.6	2.0	2.0	2.0
	max duct., $\mu_{d,max}$ [%]	1.9	2.2	2.4	2.4	2.7	3.1	3.4	4.0	4.0
	min damp., $\xi_{d,min}$ [%]	9.5	9.8	9.8	9.6	9.5	9.8	12.0	12.2	12.5
	max damp., $\xi_{d,max}$ [%]	11.6	12.7	13.5	13.5	14.5	15.3	15.9	16.9	17.0
	min b. shear [kN]	2246	2399	2527	2385	2500	2604	2615	2726	3275
	max b. shear [kN]	3361	4157	5144	5044	6492	7525	5605	7023	8160

Table 7 Maximum interstorey drift and floor acceleration values (referring to maximum/minimum ductility) for the Servitiability (Tr = 50 years) and Ultimate limit state (Tr = 475 years) for all the building configurations and seismicity levels

			FBD—Traditional								
			Low seismicity			Moderate seismicity			High seismicity		
Importance class			II	III	IV	II	III	IV	II	III	IV
Frame	SLS	min drift, θ_{min} [%]	0.41	0.47	0.54	0.35	0.42	0.45	0.41	0.47	0.54
		max drift, θ_{max} [%]	0.46	0.57	0.62	0.37	0.47	0.51	0.46	0.57	0.62
		min floor accel., a_{min} [g]	0.61	0.84	1.04	0.49	0.63	0.79	0.61	0.84	1.04
		max floor accel., a_{max} [g]	0.54	0.70	0.72	0.47	0.56	0.69	0.54	0.70	0.72
	ULS	min drift, θ_{min} [%]	1.14	1.16	1.25	0.93	1.0	0.98	1.14	1.16	1.25
		max drift, θ_{max} [%]	1.29	1.47	1.63	0.93	1.05	1.11	1.29	1.47	1.63
		min floor accel., a_{min} [g]	1.24	1.29	1.53	1.14	1.27	1.24	1.24	1.29	1.53
		max floor accel., a_{max} [g]	0.80	0.78	0.83	0.90	0.83	0.83	0.8	0.78	0.83
Wall	SLS	min drift, θ_{min} [%]	0.35	0.42	0.49	0.30	0.36	0.41	0.35	0.42	0.49
		max drift, θ_{max} [%]	0.41	0.48	0.56	0.34	0.42	0.49	0.41	0.48	0.56
		min floor accel., a_{min} [g]	0.94	1.25	1.52	0.75	0.95	1.14	0.94	1.25	1.52
		max floor accel., a_{max} [g]	0.81	1.09	1.32	0.67	0.82	0.96	0.81	1.09	1.32
	ULS	min drift, θ_{min} [%]	0.90	0.96	1.02	0.76	0.85	0.86	0.90	0.96	1.02
		max drift, θ_{max} [%]	1.04	1.02	1.11	0.80	0.88	0.93	1.04	1.02	1.11
		min floor accel., a_{min} [g]	2.32	2.81	3.12	1.91	2.22	2.36	2.32	2.81	3.12
		max floor accel., a_{max} [g]	1.54	2.23	2.43	1.52	1.49	1.74	1.54	2.23	2.43
			DDBD—traditional								
			Low seismicity			Moderate seismicity			High seismicity		
Importance class			II	III	IV	II	III	IV	II	III	IV
Frame	SLS	min drift, θ_{min} [%]	0.32	0.40	0.39	0.40	0.48	0.51	0.45	0.50	0.56
		max drift, θ_{max} [%]	0.35	0.46	0.47	0.49	0.56	0.56	0.54	0.58	0.65
		min floor accel., a_{min} [g]	0.36	0.45	0.61	0.48	0.61	0.78	0.63	0.9	1.12
		max floor accel., a_{max} [g]	0.33	0.39	0.44	0.39	0.45	0.50	0.47	0.49	0.56
	ULS	min drift, θ_{min} [%]	0.87	0.96	0.91	1.0	1.08	1.1	1.24	1.26	1.3
		max drift, θ_{max} [%]	0.97	1.10	1.2	1.29	1.42	1.5	1.67	2.03	2.07
		min floor accel., a_{min} [g]	0.60	0.64	0.84	0.71	0.85	0.94	1.02	1.18	1.5
		max floor accel., a_{max} [g]	0.43	0.47	0.49	0.44	0.49	0.54	0.55	0.54	0.65
Wall	SLS	min drift, θ_{min} [%]	0.30	0.39	0.42	0.39	0.46	0.52	0.44	0.51	0.58
		max drift, θ_{max} [%]	0.36	0.46	0.51	0.48	0.56	0.62	0.54	0.59	0.65
		min floor accel., a_{min} [g]	0.44	0.53	0.68	0.58	0.74	0.90	0.74	1.03	1.28
		max floor accel., a_{max} [g]	0.37	0.46	0.51	0.47	0.50	0.52	0.55	0.70	0.82
	ULS	min drift, θ_{min} [%]	0.80	0.86	0.88	0.88	0.93	0.99	1.07	1.09	1.15
		max drift, θ_{max} [%]	0.91	1.04	1.18	1.18	1.36	1.56	1.59	1.59	1.66
		min floor accel., a_{min} [g]	0.86	0.94	1.15	1.10	1.26	1.42	1.43	1.83	2.11
		max floor accel., a_{max} [g]	0.63	0.68	0.70	0.65	0.69	0.71	0.79	1.03	1.21

Table 7 (continued)

			DDBD–low damage								
			Low seismicity			Moderate seismicity			High seismicity		
Importance class			II	III	IV	II	III	IV	II	III	IV
Frame	SLS	min drift, θ_{min} [%]	0.27	0.40	0.40	0.40	0.40	0.53	0.53	0.66	0.66
		max drift, θ_{max} [%]	0.40	0.40	0.53	0.40	0.53	0.53	0.53	0.66	0.80
		min floor accel., a_{min} [g]	0.38	0.48	0.57	0.51	0.64	0.76	0.57	0.72	0.88
		max floor accel., a_{max} [g]	0.33	0.36	0.38	0.36	0.38	0.40	0.38	0.41	0.44
	ULS	min drift, θ_{min} [%]	0.93	0.93	1.06	1.06	1.19	1.33	1.46	1.59	1.72
		max drift, θ_{max} [%]	0.93	1.19	1.33	1.33	1.46	1.72	1.86	2.12	2.52
		min floor accel., a_{min} [g]	0.62	0.77	0.95	0.86	1.09	1.26	0.75	0.92	1.13
		max floor accel., a_{max} [g]	0.41	0.44	0.46	0.44	0.46	0.48	0.49	0.51	0.55
Wall	SLS	min drift, θ_{min} [%]	0.15	0.15	0.15	0.15	0.15	0.31	0.15	0.31	0.31
		max drift, θ_{max} [%]	0.15	0.15	0.31	0.31	0.31	0.31	0.31	0.46	0.46
		min floor accel., a_{min} [g]	0.69	0.84	1.04	1.02	1.29	1.54	1.07	1.37	1.64
		max floor accel., a_{max} [g]	0.45	0.49	0.51	0.48	0.50	0.52	0.50	0.52	0.64
	ULS	min drift, θ_{min} [%]	0.61	0.61	0.61	0.61	0.61	0.61	0.77	0.92	0.92
		max drift, θ_{max} [%]	0.61	0.77	0.92	0.92	1.07	1.23	1.38	1.69	1.84
		min floor accel., a_{min} [g]	0.79	0.97	1.19	1.18	1.49	1.76	1.30	1.63	1.92
		max floor accel., a_{max} [g]	0.53	0.57	0.60	0.57	0.60	0.62	0.62	0.64	0.78

Acknowledgements The authors acknowledge the financial support of the Italian Ministry of Education, University and Research (MIUR) for funding the Doctoral Scholarships of Jonathan Ciurlanti. The authors also acknowledge the funding from the European Union's Horizon 2020 research and innovation programme under the Marie Skłodowska-Curie grant agreement No. 101029605 (H2020-MSCA-IF-2020—SAFE-FACE—Seismic SAFety and Energy efficiency: Integrated technologies and multi-criteria performance-based design for building FACadEs) for Simona Bianchi. Furthermore, the authors acknowledge Francesca Gentili for her contribution to the initial feasibility study, as part of her Master's Thesis at Sapienza University of Rome, and the contribution of Giovanni Milan from ARUP Netherlands in supporting the development of the machine learning algorithm.

Authors' contribution JC, SB: Conceptualization, Investigation, Project administration, Formal analysis, Data curation, Writing—Original Draft, Visualization. SP: Conceptualization, Supervision, Writing—Review & Editing.

Funding Italian Ministry of Education, University and Research (MIUR) for funding the Doctoral Scholarship of Jonathan Ciurlanti; European Union's Horizon 2020 research and innovation programme under the Marie Skłodowska-Curie grant agreement No. 101029605 for funding Simona Bianchi.

Availability of data and material The raw data gathered during the tests is available upon request.

Declarations

Conflicts of interest There is no conflict of interest.

Consent to participate All the authors agreed to participate in the writing of this manuscript.

Consent to publication All the authors agreed to submit this manuscript.

References

ATC 40 (1996) Seismic evaluation and retrofit of concrete buildings, Volume 1. Redwood City, California, USA.

Baird A, Palermo A, Pampanin S (2013) Controlling seismic response using passive energy dissipating cladding connections. 2013 NZSEE Conference, Wellington, New Zealand

Benavent-Climent A, Donaire-Ávila J, Mollaioli F (2021) Key points and pending issues in the energy-based seismic design approach. In: Benavent-climent A, Mollaioli F (eds) Energy-based seismic engineering. IWEBSE 2021. Lecture Notes in civil engineering, vol 155. Springer, Cham. https://doi.org/10.1007/978-3-030-73932-4_11

Bianchi S, Pampanin S (2022) Fragility functions for architectural nonstructural components. J Struct Eng. https://doi.org/10.1061/(ASCE)ST.1943-541X.0003352

Bianchi S, Ciurlanti J, Pampanin S (2020) Comparison of traditional vs low-damage structural & non-structural building systems through a cost/performance-based evaluation. Earthq Spectra. https://doi.org/10.1177/8755293020952445

Bianchi S, Ciurlanti J, Perrone D, Filiatrault A, Costa AC, Candeias PX, Correia AP, Pampanin S (2021) Shake-table tests of innovative drift sensitive nonstructural elements in a low-damage structural system. Earthq Eng Struct Dyn 50(9):2398–2420. https://doi.org/10.1002/eqe.3452

Bianchi S, Ciurlanti J, Overend M, Pampanin S (2022) A probabilistic-based framework for the integrated assessment of seismic and energy economic losses of buildings. Eng Struct. https://doi.org/10.1016/j.engstruct.2022.114852

Brandolese S, Fiorin L, Scotta R (2019) Seismic demand and capacity assessment of suspended ceiling systems. Eng Struct 193:219–237. https://doi.org/10.1016/j.engstruct.2019.05.034

Carr AJ (2003) Ruaumoko program for inelastic dynamic analysis—user manual. University of Canterbury, Christchurch, NZ

Ciurlanti J, Bianchi S, Pürgstaller A, Quintana-Gallo P, Bergemeister K, Pampanin S (2022) Shake table tests of concrete anchors for non-structural components including innovative and alternative anchorage detailing. Bull Earthq Eng. https://doi.org/10.1007/s10518-022-01359-2

Cornell CA, Jalayer F, Hamburger RO, Foutch DA (2002) Probabilistic basis for 2000 SAC federal emergency management agency steel moment frame guidelines. J Struct Eng 128(4):526–533. https://doi.org/10.1061/(ASCE)0733-9445(2002)128:4(526)

DEI (2012) Prezzi per tipologie edilizie, tipografia del genio civile, collegio degli ingegneri ed architetti di Milano, Milano, IT

Dhakal RP, MacRae GA, Pourali A, Paganotti G (2016) Seismic fragility of suspended ceiling systems used in NZ based on component tests. Bull NZ Soc Earthq Eng 49(1):46–63. https://doi.org/10.5459/bnzsee.49.1.45-63

DM 58 (2017) Ministero delle Infrastrutture. Linee guida per la classificazione del rischio sismico delle costruzioni, Decreto Ministeriale 58 del 28/02/2017, Rome, IT

DPCM (2018) Prezziario unico del cratere del centro italia. presidenza del consiglio dei ministri, ordinanza n. 58 del Commissario del Governo per la ricostruzione del 4/07/2018

EN 1998–1 (2004) Eurocode 8: design of structures for earthquake resistance—part 1: general rules, seismic actions and rules for buildings. European Committee for Standardization (CEN), Brussels, Belgium

Fardis M (2018) From force- to displacement-based seismic design of concrete structures and beyond. In: 16th European conference on earthquake engineering, Thessaloniki, Greece

FEMA P-58–1 (2018) Seismic performance assessment of buildings, volume 1—methodology. Applied technology council for the federal emergency management agency, Washington, USA.

FEMA P-58–7 (2018) seismic performance assessment of buildings, Volume 7—a guide to state-of-the-art tools for seismic design and assessment. Applied technology council for the federal emergency management agency, Washington, USA

fib (2003) Bulletin No. 27. International federation for structural concrete, Lausanne, CHE

Gentili F, Ciurlanti J, Bianchi S, Pampanin S (2021) Exploring the expected increase of costs and loss reduction by raising the bar in seismic design: comparison of alternative design methodologies and earthquake-resistant technologies. 8th COMPDYN Conference, Athens, GR.

Gunay S, Mosalam KM (2013) PEER performance-based earthquake engineering methodology revisited. J Earthq Eng 17:829–858. https://doi.org/10.1080/13632469.2013.787377
Johnston HC, Watson CP, Pampanin S, Palermo A (2014) Shake table testing of an integrated low-damage frame building. In: NZSEE Conference, Auckland, NZ
Kam WY, Pampanin S, Elwood KJ (2011) Seismic performance of reinforced concrete buildings in the 22 February Christchurch (Lyttelton) earthquake. Bull NZ Soc Earthq Eng 44(4):239–278. https://doi.org/10.5459/bnzsee.44.4.239-278
Kasai K, Nakai M, Nakamura Y, Asai H, Suzuki Y, Ishii M (2009) Building passive control in Japan. J Disaster Res 4(3):261
Krawinkler H, Miranda E (2004) Performance-based earthquake engineering. In: Bertero VV (ed) Earthquake engineering: from engineering seismology to performance-based engineering. CRC Press, Boca Raton
Marriott D, Pampanin S, Bull D, Palermo A (2008) Dynamic testing of precast, post-tensioned rocking wall systems with alternative dissipating solutions. Bull NZ Soc Earthq Eng 41(2):90–103
McNeel R et al (2010) Rhinoceros 3D, version 6.0. Robert McNeel & associates, Seattle, USA
Newcombe MP, Pampanin S, Buchanan A, Palermo A (2008) Section analysis and cyclic behavior of post-tensioned jointed ductile connections for multi-storey timber buildings. J Earthq Eng 12(S1):83–110
NTC (2018) Aggiornamento delle norme tecniche per le costruzioni, supplemento ordinario n°8 alle G.U. n° 42 del 20/02/2018. Ministero delle Infrastrutture, Rome, IT
NZS 1170.5 (2004) Structural design actions—Part 5: earthquake actions. NZS 1170.5. Wellington, NZ
O'Reilly GJ, Perrone D, Fox M, Monteiro R, Filiatrault A (2018) Seismic assessment and loss estimation of existing school buildings in Italy. Eng Struct 168(1):142–162
Pampanin S (2005) Emerging solutions for high seismic performance of precast -prestressed concrete buildings. J AdvConcr Technol 3(2):202–222
Pampanin S (2012) Reality-check and renewed challenges in earthquake engineering: implementing low-damage structural systems—from theory to practice. Bull NZ Soc Earthq Eng 45(4):137–160
Pampanin S (2015) Towards the "ultimate earthquake-proof" building: development of an integrated low-damage system. In: Ansal A (ed) Perspectives on European earthquake engineering and seismology, geotechnical, geological and earthquake engineering 39. Springer, Cham
Pampanin S, Priestley MJN, Sritharan S (2001) Analytical modeling of the seismic behavior of precast concrete frames designed with ductile connections. J Earthq Eng 5(3):329–367. https://doi.org/10.1080/13632460109350397
Pampanin S, Marriott D, Palermo A, NZ Concrete Society (2010) PRESSS design handbook. Auckland, NZ
Pourali A, Dhakal RP, MacRae GA, Tasligedik AS (2017) Fully-floating suspended ceiling system: experimental evaluation of the effect of mass and elastic isolation. In: 16th world conference on earthquake engineering. Santiago, Chile
Priestley MJN (1991) Overview of PRESSS research Program. PCI J 36(4):50–57
Priestley MJN (1998) Displacement-based approaches to rational limit states design of new structures. In: 11th European conference on earthquake engineering. Paris, FR
Priestley MJN (2003) Myths and fallacies in earthquake engineering. IUSS Press, Pavia, IT, Revisited. Mallet Milne Lecture
Priestley MJN, Kowalsky MJ (2000) Direct displacement-based seismic design of concrete buildings. Bull NZ Soc Earthq Eng 33(4):421–444
Priestley MJN, Calvi MC, Kowalsky MJ (2007) Displacement-based seismic design of structures. IUSS Press, Pavia, IT, p 670
Priestley MJN, Sritharan S, Conley JR, Pampanin S (1999) Preliminary results and conclusions from the PRESSS five-story precast concrete test building. PCI J 44(6):42–67
Priestley MJN, Grant DN, Blandon C (2005) Direct displacement-based seismic design. In: 2005 NZSEE conference, Auckland, NZ
Ricci P, De Luca F, Verderame GM (2011) 6th April 2009 L'Aquila earthquake, Italy: reinforced concrete building performance. Bull Earthq Eng 9:285–305. https://doi.org/10.1007/s10518-010-9204-8
Ricles JM, Christopoulos C, Sause R, Garlock ME (2010) Development of self-centering steel moment-resisting frames for damage-free seismic resistant buildings. In: 9th US national and 10th canadian conference on earthquake engineering, Toronto, Canada
Sarti F, Palermo A, Pampanin S (2016) Fuse-type external replaceable dissipaters: experimental program and numerical modeling. J Struct Eng 142:12. https://doi.org/10.1061/(ASCE)ST.1943-541X.0001606
Sporn B, Pampanin S (2013) A "retrofit" solution for force-based design: eliminating the need for iteration and initial period estimation. In: 2013 NZSEE Conference, Wellington, NZ
Sullivan TJ (2013) Highlighting differences between force-based and displacement-based design solutions for reinforced concrete frame structures. Struct Eng Int. https://doi.org/10.2749/101686613X13439149156958

Taghavi S and Miranda E (2003) Response assessment of nonstructural building elements. In: Pacific earthquake engineering research center, Berkley, California, USA

Tasligedik AS, Pampanin S (2016) Rocking cantilever clay brick infill wall panels: a novel low damage infill wall system. J Earthq Eng 21(7):1023–1049. https://doi.org/10.1080/13632469.2016.1190797

Tasligedik AS, Pampanin S, Palermo A (2015) Low damage seismic solutions for non-structural drywall partitions. Bull Earthquake Eng 13:1029–1050. https://doi.org/10.1007/s10518-014-9654-5

Verderame GM, Iervolino I, Ricci P (2009) Report on the damages on buildings following the seismic event of 6th of April 2009 time 1.32 (UTC)—L'Aquila M=5.8, V1.20

Wallace JW, Massone LM, Bonelli P, Dragovich J, Lagos R, Lüders C, Moehle J (2012) Damage and implications for seismic design of RC structural wall buildings. Earthq Spectra 28:281–299

Whittaker A, Soong TT (2003). An overview of nonstructural research at three U.S. Earthquake engineering research centers, In: ATC-29–2 seminar on the seismic design, performance and retrofit of nonstructural components in critical facilities, Irvine, California

Zsarnóczay A, Deierlein GG (2020) Pelicun - a computational framework for estimating damage, loss and community resilience. In: 17th world conference of earthquake engineering, Sendai, JP